# MID-AMERICA TRANSPORTATION CENTER

Report # MATC-UNL: 004-15

Final Report

## Investigation and Development of a MASH Test Level 6, Cost-Effective Barrier System for Containing Heavy Tractor Tank-Trailer Vehicles and Mitigating Catastrophic Crash Events - Phase V

**Cody S. Stolle, PhD**
Research Assistant Professor
Department of Civil & Environmental Engineering
Midwest Roadside Safety Facility
The University of Nebraska-Lincoln

**Ronald K. Faller, PhD, PE**
Research Professor & MwRSF Director

**Scott Rosenbaugh, MSCE**
Research Engineer

**Andrew E. Loken, PhD**
Research Assistant Professor

**Robert Bielenberg, MSME**
Research Engineer

**Joshua S. Steelman, PhD, PE**
Associate Professor

2024

A Cooperative Research Project sponsored by U.S. Department of Transportation- Office of the Assistant Secretary for Research and Technology

University of Nebraska–Lincoln

The University of Iowa

KU The University of Kansas

Missouri S&T

Lincoln University Missouri

Nebraska Indian Community College

University of Nebraska Omaha

University of Nebraska Medical Center

KU Medical Center The University of Kansas

Investigation and Development of a MASH Test Level 6, Cost-Effective Barrier System for Containing Heavy Tractor Tank-Trailer Vehicles and Mitigating Catastrophic Crash Events – Phase V

Alternate Title: High-Performance, Single-Slope Concrete Barrier - Height Transition and Foundation Considerations

Cody S. Stolle, Ph.D.
Research Assistant Professor

Scott Rosenbaugh, M.S.C.E.
Research Engineer

Andrew E. Loken, Ph.D.
Research Assistant Professor

Ronald K. Faller, Ph.D., P.E.
Research Professor & MwRSF Director

Robert Bielenberg, M.S.M.E.
Research Engineer

Joshua S. Steelman, Ph.D., P.E.
Associate Professor

A Report on Research Performed by

Midwest Roadside Safety Facility
Nebraska Transportation Center
University of Nebraska-Lincoln

August 7, 2024

TECHNICAL REPORT DOCUMENTATION PAGE

| 1. Report No.<br>25-1121-0005-004-15 | 2. Government Accession No. | 3. Recipient's Catalog No. |
|---|---|---|
| **4. Title and Subtitle**<br>Investigation and Development of a MASH Test Level 6, Cost-Effective Barrier System for Containing Heavy Tractor Tank-Trailer Vehicles and Mitigating Catastrophic Crash Events – Phase V | **5. Report Date**<br>August 7, 2024 | |
| | **6. Performing Organization Code** | |

| **7. Author(s)**<br>Stolle, C.S., Faller, R.K., Rosenbaugh, S.K., Bielenberg, R.W., Loken, A.E., and Steelman, J.S. | **8. Performing Organization Report No.**<br>25-1121-0005-004-15 |
|---|---|

| **9. Performing Organization Name and Address**<br>Midwest Roadside Safety Facility (MwRSF)<br>Nebraska Transportation Center<br>University of Nebraska-Lincoln | **10. Work Unit No.** |
|---|---|
| Main Office:<br>Prem S. Paul Research Center at Whittier School<br>Room 130, 2200 Vine Street<br>Lincoln, Nebraska 68583-0853    Outdoor Test Site:<br>4630 N.W. 36th Street<br>Lincoln, Nebraska 68524 | **11. Contract**<br>69A3551747107 |

| **12. Sponsoring Agency Name and Address**<br>Mid-American Transportation Center<br>2200 Vine Street<br>Lincoln, Nebraska 68583 | **13. Type of Report and Period Covered**<br>Final Report: 2021-2024 |
|---|---|
| | **14. Sponsoring Agency Code**<br>TRB RiP# 91994-102 |

**15. Supplementary Notes**

Prepared in cooperation with U.S. Department of Transportation, Federal Highway Administration

**16. Abstract**

U.S. roads carry a mix of motor-vehicle traffic, including motorcycles, passenger vehicles, buses, trucks, recreational vehicles, and other specialized vehicles. Occasionally, tractor-tank trailer vehicles become errant, depart their intended travel lanes, and become run-off-road events. Most highway barrier systems are not intended to prevent penetration and override by high-energy crashes with tractor-tank trailer vehicles. This multi-year, research study developed an optimized barrier to contain and redirect crashes with tractor-tank trailer vehicles under TL-6 impact conditions in AASHTO's *Manual for Assessing Safety Hardware* (MASH).

A 62-in. tall, 5.5-degree, single-slope, concrete barrier was configured using yield-line analysis procedures and a 300-kip design lateral load distributed at two heights. The barrier system incorporated top and bottom widths of 10 in. and 22 in., respectively, and utilized a ¾-in. wide expansion gap. One crash test with an 80,026-lb 2010 Columbia 112 Freightliner tractor with 1997 LBT tank trailer was performed using a tractor-tank trailer impacting the barrier system at 51.1 mph and 15.7 degrees under MASH test 6-12. The barrier successfully contained and redirected the tractor-tank trailer without barrier penetration or override. Upon exit, the vehicle rolled 90 degrees and slid on the concrete tarmac through 6.5 seconds. The vehicle with oval-shaped tank and sloshing liquid cargo traversed the concrete tarmac and began to roll another 180 degrees, whereby crush occurred to the truck's cab. Minimal damage occurred to the barrier system. Through 6.5 seconds, the MASH TL-6 barrier system contained and redirected the vehicle with roll onto its side and with all occupant risk criteria met. Design concepts for height transitions and alternative foundations were prepared to assist with future system implementation in high-risk areas where tractor-tank trailer vehicle protection is desired. Further discussion is recommended to determine proper crash test expectations for TL-6 barriers under high-energy impact events with round- and oval-tank trailers.

| **17. Key Words**<br>MASH TL-6, Highway Safety, Crash Test, Roadside Appurtenances, Compliance Test, MASH 2016, Single-Slope Concrete Barrier, Median, Roadside, Height Transitions, and Foundations | **18. Distribution Statement**<br>No restrictions. This document is available through the National Technical Information Service.<br>5285 Port Royal Road<br>Springfield, VA 22161 | | |
|---|---|---|---|
| **19. Security Classification (of this report)**<br>Unclassified | **20. Security Classification (of this page)**<br>Unclassified | **21. No. of Pages**<br>66 | **22. Price** |

**Form DOT F 1700.7 (8-72)**      Reproduction of completed page authorized

Disclaimer Statement

This material is based upon work supported by the Mid-America Transportation Center (MATC), U.S. Department of Transportation (USDOT) Region VII University Transportation Center (UTC). This report was completed with funding from the Mid-America Transportation Center (MATC), a US Department of Transportation (USDOT) Region VII University Transportation Center (UTC). The contents of this report reflect the views and opinions of the authors who are responsible for the facts and the accuracy of the data presented herein. The contents do not necessarily reflect the official views or policies of MATC, USDOT, nor the Federal Highway Administration (FHWA). This report does not constitute a standard, specification, regulation, product endorsement, or an endorsement of manufacturers.


Uncertainty of Measurement Statement

The Midwest Roadside Safety Facility (MwRSF) has determined the uncertainty of measurements for several parameters involved in standard full-scale crash testing and non-standard testing of roadside safety features. Information regarding the uncertainty of measurements for critical parameters is available upon request by the sponsor and the Federal Highway Administration.

Acknowledgements

| SI* (Modern Metric) Conversion Factors | | | | |
|---|---|---|---|---|
| **APPROXIMATE CONVERSIONS TO SI UNITS** | | | | |
| **Symbol** | **When You Know** | **Multiply By** | **To Find** | **Symbol** |
| **LENGTH** | | | | |
| in. | inches | 25.4 | millimeters | mm |
| ft | feet | 0.305 | meters | m |
| yd | yards | 0.914 | meters | m |
| mi | miles | 1.61 | kilometers | km |
| **AREA** | | | | |
| $in^2$ | square inches | 645.2 | square millimeters | $mm^2$ |
| $ft^2$ | square feet | 0.093 | square meters | $m^2$ |
| $yd^2$ | square yard | 0.836 | square meters | $m^2$ |
| ac | acres | 0.405 | hectares | ha |
| $mi^2$ | square miles | 2.59 | square kilometers | $km^2$ |
| **VOLUME** | | | | |
| fl oz | fluid ounces | 29.57 | milliliters | mL |
| gal | gallons | 3.785 | liters | L |
| $ft^3$ | cubic feet | 0.028 | cubic meters | $m^3$ |
| $yd^3$ | cubic yards | 0.765 | cubic meters | $m^3$ |
| NOTE: volumes greater than 1,000 L shall be shown in $m^3$ | | | | |
| **MASS** | | | | |
| oz | ounces | 28.35 | grams | g |
| lb | pounds | 0.454 | kilograms | kg |
| T | short ton (2,000 lb) | 0.907 | megagrams (or "metric ton") | Mg (or "t") |
| **TEMPERATURE (exact degrees)** | | | | |
| °F | Fahrenheit | 5(F-32)/9 or (F-32)/1.8 | Celsius | °C |
| **ILLUMINATION** | | | | |
| fc | foot-candles | 10.76 | lux | lx |
| fl | foot-Lamberts | 3.426 | candela per square meter | $cd/m^2$ |
| **FORCE & PRESSURE or STRESS** | | | | |
| lbf | poundforce | 4.45 | newtons | N |
| $lbf/in^2$ | poundforce per square inch | 6.89 | kilopascals | kPa |
| **APPROXIMATE CONVERSIONS FROM SI UNITS** | | | | |
| **Symbol** | **When You Know** | **Multiply By** | **To Find** | **Symbol** |
| **LENGTH** | | | | |
| mm | millimeters | 0.039 | inches | in. |
| m | meters | 3.28 | feet | ft |
| m | meters | 1.09 | yards | yd |
| km | kilometers | 0.621 | miles | mi |
| **AREA** | | | | |
| $mm^2$ | square millimeters | 0.0016 | square inches | $in^2$ |
| $m^2$ | square meters | 10.764 | square feet | $ft^2$ |
| $m^2$ | square meters | 1.195 | square yard | $yd^2$ |
| ha | hectares | 2.47 | acres | ac |
| $km^2$ | square kilometers | 0.386 | square miles | $mi^2$ |
| **VOLUME** | | | | |
| mL | milliliter | 0.034 | fluid ounces | fl oz |
| L | liters | 0.264 | gallons | gal |
| $m^3$ | cubic meters | 35.314 | cubic feet | $ft^3$ |
| $m^3$ | cubic meters | 1.307 | cubic yards | $yd^3$ |
| **MASS** | | | | |
| g | grams | 0.035 | ounces | oz |
| kg | kilograms | 2.202 | pounds | lb |
| Mg (or "t") | megagrams (or "metric ton") | 1.103 | short ton (2,000 lb) | T |
| **TEMPERATURE (exact degrees)** | | | | |
| °C | Celsius | 1.8C+32 | Fahrenheit | °F |
| **ILLUMINATION** | | | | |
| lx | lux | 0.0929 | foot-candles | fc |
| $cd/m^2$ | candela per square meter | 0.2919 | foot-Lamberts | fl |
| **FORCE & PRESSURE or STRESS** | | | | |
| N | newtons | 0.225 | poundforce | lbf |
| kPa | kilopascals | 0.145 | poundforce per square inch | $lbf/in^2$ |

*SI is the symbol for the International System of Units. Appropriate rounding should be made to comply with Section 4 of ASTM E380.

Table of Contents

List of Figures

Chapter 1 Introduction

1.1 Background

Our nation's road network was designed to carry a mix of motor-vehicle traffic, ranging from motorcycles, passenger vehicles, buses, trucks, recreational vehicles, and other specialized vehicles and equipment. For the daily transport of freight, several types and sizes of commercial vehicles are found on the roadway system, including single-unit trucks and tractor-trailer trucks. For the tractor-trailer vehicles, a wide variety of semi-trailers have existed, such as those often termed as flatbed, step/drop deck, lowboy, reefer, dump, tipper, dry van, and tanker. The tanker or tank trailers have largely been used for the transport of food products, fuels, chemicals, waste products, or other hazardous materials.

Each day and across U.S. highways and roadways, numerous vehicles become errant and encroach into adjacent travel lanes, oncoming traffic, paved shoulders, as well as roadsides and medians. For those lane departures that result in run-off-road (ROR) events, it is common practice for longitudinal barriers (i.e., guardrails, median barriers, and bridge railings) to be implemented to prevent errant motorists from striking hazardous fixed objects or geometric features, thus mitigating the risk and severity of those ROR crash events. For most road scenarios, it has been appropriate to utilize barrier systems that are capable of safely containing and redirecting most passenger vehicles. Most barrier systems have generally met the Test Level 3 (TL-3) safety performance guidelines published in the National Cooperative Highway Research Program (NCHRP) Report 350, *Recommended Procedures for the Safety Performance Evaluation of Highway Features* [1] or the American Association of State Highway and Transportation Officials (AASHTOs) *Manual for Assessing Safety Hardware* [2-3].

It has been deemed necessary to use higher-performance, vehicle containment systems (i.e., TL-4 through TL-6) to shield fixed obstacles and hazards located within roadsides and

medians when (1) the roadway has a high percentage of truck and other heavy vehicle traffic and/or (2) the consequences of vehicle penetration beyond the longitudinal barrier is too great. Across the U.S., TL-4 and TL-5 barriers have historically been implemented when considerations exist for truck and other heavy vehicle traffic. These TL-4 and TL-5 barriers have been crash-tested and evaluated using either single-unit truck or tractor-van trailer vehicles.

Tractor-tank trailers also exist on our nation's road network, which occasionally become errant and depart their intended travel lanes. When tractor-tank trailers become ROR events, the existing barrier systems may not be able to adequately capture those heavy vehicles impacting at higher speeds and angles. Tractor-tank trailers often have higher centers of mass and exhibit reduced stability as compared to other commercial vehicles. When tractor-tank trailers impact roadside infrastructure, the increased height of the mass can provide increased structural demand to the barrier's base. In other words, many TL-4 and TL-5 barriers may be structurally inadequate and have insufficient height to safely contain and redirect tractor-tank trailers departing at an extreme design impact condition. When containment barriers are inadequate, there are elevated risks of serious injuries, fatalities, damaged infrastructure, and even traffic delays. Further, these scenarios can pose catastrophic consequences to opposing traffic, high-risk facilities, and highly-populated urban/suburban areas, especially when errant tractor-tank trailers are transporting fuels, chemicals, or other hazardous materials.

Thus far, only one TL-6 barrier was successfully developed and crash tested, and it was evaluated by Texas A&M Transportation Institute (TTI) researchers according to prior impact safety standards using a tractor-tank trailer [4]. This combination barrier configuration, often referred to as the *Roman Wall*, consisted of a lower solid concrete parapet with an upper concrete beam and post railing system, and it measured approximately 90 in. tall, as shown in Figure 1.1 and Figure 1.2. Note that the Roman Wall was crash tested before the publication of NCHRP

Report 350 [1] and MASH [2-3]. However, the impact conditions and vehicle geometry were comparable used for NCHRP Report 350 and MASH TL-6 tractor-tank trailer vehicles.





Figure 1.1 90-in. Tall, Combination Barrier System for Tractor-Tank Trailer Impact Events [4]

[Photographs courtesy of Texas A&M Transportation Institute]
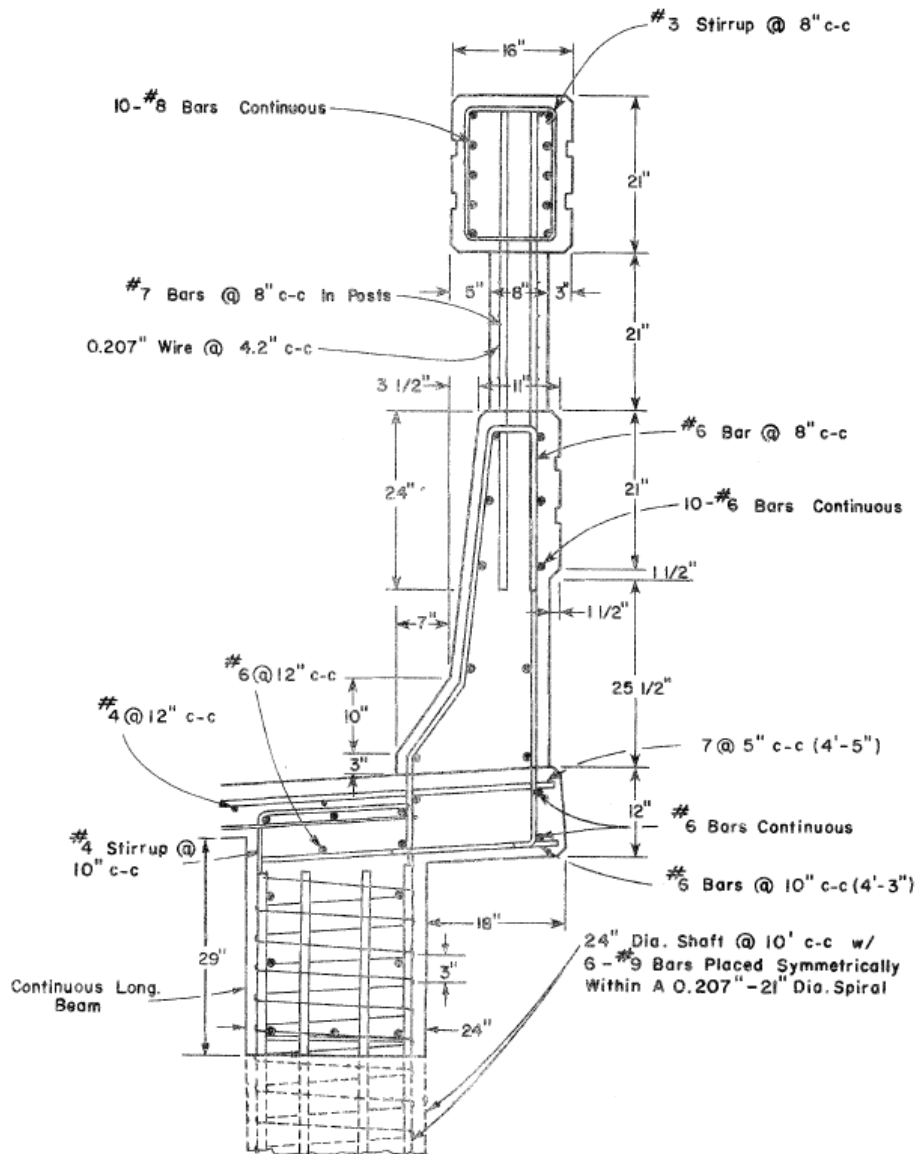
Figure 1.2 TTI 90-in. Tall, TL-6 Roman Wall Design Details [4]

Unfortunately, the installation cost and overall height of this robust, TL-6 containment barrier may have limited its implementation to a small number of sites across the U.S. A few real-world installations are shown in Figure 1.3. As a result, there remain numerous locations where crash protection and vehicle containment against tractor-tank trailer vehicles may be desired. These situations would consider (1) prevention and mitigation of tractor-tank trailer

vehicles involved in cross-median, opposing-traffic crashes on urban freeways and interstates or (2) penetration through or override of existing TL-3, TL-4, or TL-5 barriers located on bridges, elevated road structures, or high volume roadways, which create potential catastrophic events near schools, malls, sports venues, concert arenas, military bases, international airports, critical government buildings, or other high-risk facilities. As such, there existed a need to develop, a new, optimized, structurally-adequate, reduced-height, vehicle containment system to contain errant vehicle impacts with heavy tractor-tank trailers to prevent or mitigate the consequences of catastrophic crashes into opposing traffic, high-risk facilities, and highly-populated areas.
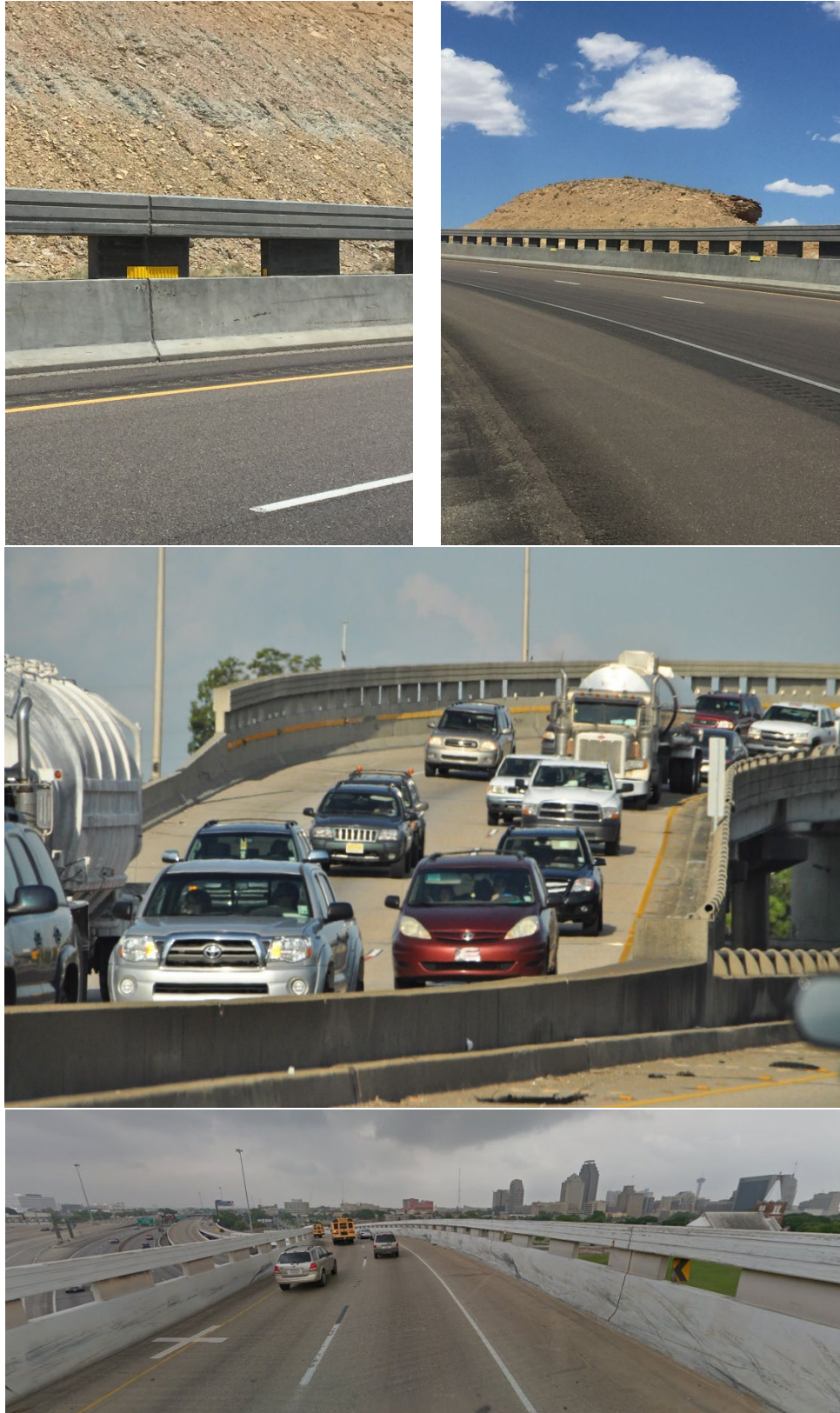
Figure 1.3 TL-6 Roman Wall Installations - Utah (top), Louisiana (middle), and Texas (bottom)

1.2 Literature Review

A cross-sectional study of commercial truck crashes in Tennessee between 2006 and 2010 identified 5,650 truck-involved crashes, including 218 severe crashes (K+A), and indicated that increases in AADT as well as increases in corresponding truck percentages resulted in higher frequencies of heavy truck crashes [5]. Researchers have also noted that tractor-tank trailer vehicle crashes may cause significant damage to transportation infrastructure as well as present crash and injury risk to adjacent traffic. Shen et al [6] reviewed tractor-tank trailer crashes involving hazardous materials transport in China between 2004 and 2011 and observed that the most common crash outcomes were rollovers (29.1%), ROR crashes (16.7%), and rear-end collisions (13.3%). Further, McKnight and Bahouth performed detailed forensic evaluation of 231 large truck rollover crashes, and identified that significant contributors to crashes were failing to adjust speed on roadway curves and intersections, driver inattention (i.e., distracted driving or drowsiness), and maneuver errors, including oversteering, overcorrection, and other steering and control errors [7]. Their findings were similar to a statistical analysis of tractor-tank trailer crashes by Iranitalab, Khattak, and Bahouth [8], who also evaluated crashes in which hazardous material ("hazmat") was released. The emission of hazmat cargo can have devastating consequences. For example, one tractor-tank trailer vehicle involved in a rollover crash in China which was carrying liquified petroleum gas (LPG). This large vehicle had impacted a concrete barrier, where LPG was eventually released, resulting in a fire and vapor cloud explosion, which killed 20 people and injured 175 others in the area [9]. Additional significant anecdotal evidence of adverse outcomes resulting from tractor-tank trailer crashes are readily available. Numerous tractor-tank trailer vehicle crashes with roadside infrastructure were reviewed, and the roadside protection infrastructure was frequently inadequate to contain and redirect these large vehicles, even contributing to rollover or collision with features in the Zone of Intrusion (ZOI) [10-13].

Note that TL-6 barriers were not utilized at these locations where catastrophic had events occurred.

1.3 Research Objectives and Plan

The research objectives for this study included the development of a new, optimized, cost-effective, reinforced concrete barrier to primarily contain and redirect tractor-tank trailer vehicles according to the MASH TL-6 impact safety standards [2-3] and also safely and stably containing and redirecting passenger vehicles (i.e., small cars and pickup trucks) with acceptable levels of occupant risk. The research effort considered methods for mitigating the catastrophic risks associated with these heavy trucks to penetrate through and override the new containment barrier. One important objective included the selection of the lowest, reasonable height below the existing, 90-in. tall, *Roman Wall* to capture heavy commercial truck vehicles at the TL-6 design impact condition. The selection of a reduced-height barrier and a narrow footprint assisted in controlling construction costs. With an overall barrier height closer to heights of TL-5 barriers outfitted with upper glare screens, there would be an increased likelihood for government road authorities to utilize a new TL-6 barrier to mitigate catastrophic risks associated with crashes involving tractor-tank trailer vehicles. For this MASH TL-6 barrier, it was intended to be adaptable for use in roadside, median, and bridge deck applications, as well as terminate to connect to common crashworthy approach guardrail transitions.

During this multi-phase study, the research team reviewed the available literature as well as anecdotal reports of tractor-tank trailer vehicle crashes, including those events involving roadside safety hardware [14-15]. Selected Departments of Transportation were surveyed to garner initial feedback on preferences for the new barrier. Tractor-tank trailer manufacturers and industry sources were queried to obtain common vehicle dimensions and configurations. The researchers investigated the relationship between truck behavior and barrier height, specifically

critical barrier height, override, roll angle, vehicle stability, and vehicle-to-barrier impact loading.

This investigation also led to the development of a TL-6 tractor-tank trailer vehicle model for use in conducting computer simulations of representative vehicles impacting into barrier prototypes with varying top heights [14-18]. Finite element analysis (FEA) models were developed to represent tractor-tank trailer vehicles according to the MASH TL-6 test vehicle, a 36000T vehicle. The 36000T vehicle models were investigated and developed using test data obtained from TTI crash tests - one test into the *Roman Wall* [4] and another test into an instrumented, vertical wall [19].

Simulations of the FEA model vehicles impacting various barriers were then used to establish (1) a minimum barrier height to contain and redirect MASH TL-6 tractor-tank trailers and (2) design loads for the new barrier development [18,20]. The barrier was designed, including attachment to a rigid, unreinforced concrete foundation. A barrier configuration was selected for a full-scale crash testing to demonstrate its crashworthiness. Barrier design details were developed, and a new, optimized, barrier system was constructed at the Midwest Roadside Safety Facility's (MwRSF's) test site.

A tractor-tank trailer was acquired and prepared, and a one full-scale crash test was performed into the new barrier prototype according to MASH test designation no. 6-12 impact conditions. The full-scale vehicle crash test results were analyzed, evaluated, and documented. Conclusions and recommendations were then made pertaining to the safety performance of the TL-6 concrete barrier. General installation examples with conceptual design details were developed for addressing height transitions at the barrier ends and also alternative foundation systems to assist end users with planning for eventual implementation in areas where TL-6 tractor-tank trailer vehicle containment and redirection is desired.

This entire research study was performed over the course of several years and was supported by the Mid-America Transportation Center (MATC), a Region VII University Transportation Center (UTC) located at the University of Nebraska-Lincoln (UNL). Many of the noted tasks are briefly highlighted herein and are available in greater detail within the referenced project reports and theses [14-18,20].

Chapter 2 Overview of Barrier Development

2.1 Barrier Height and Geometry Investigation

In order to make a cost–competitive TL-6 traffic barrier, the height of the barrier was optimized. The 90-in. tall, *Roman Wall* was structurally adequate and effective in containing and redirecting tractor-tank trailer vehicles. However, it was likely not used as often by road authorities due to its construction costs to implement it in the field. A shorter barrier that was closer in height to other TL-5 barriers with glare screens would be expected to have installation costs similar to those taller TL-5 barriers, thus making the new TL-6 system more feasible to implement. On the other hand, the barrier needed to be tall enough to contain and redirect a tractor-tank trailer vehicle, thereby preventing the tank from rolling over the barrier. Thus, the barrier was designed with the minimum height required to redirect the TL-6 vehicle in order to better limit installation costs.

The effect of barrier height on the containment and redirection of a tractor-tank trailer vehicle under TL-6 impact conditions was explored through finite element analysis (FEA) using LS-DYNA. The FEA model of the MASH 36000T tractor-tank trailer vehicle was developed during previous phases of this study [14-18,20]. The tractor model was extracted from an existing TL-5 tractor-van trailer truck model, originally developed by a research team at UT-Battelle's Oak Ridge National Laboratory and the University of Tennessee at Knoxville. The FEA model of the tank trailer was based on a four-tank, elliptical shaped tank from Liquid & Bulk Tank, Inc. (LBT) and used Lagrangian Formulation to model the liquid in the tanks. The tank trailer model was developed at the MwRSF and the University of Nebraska-Lincoln. The tractor-tank trailer vehicle model is shown in Figure 2.1.
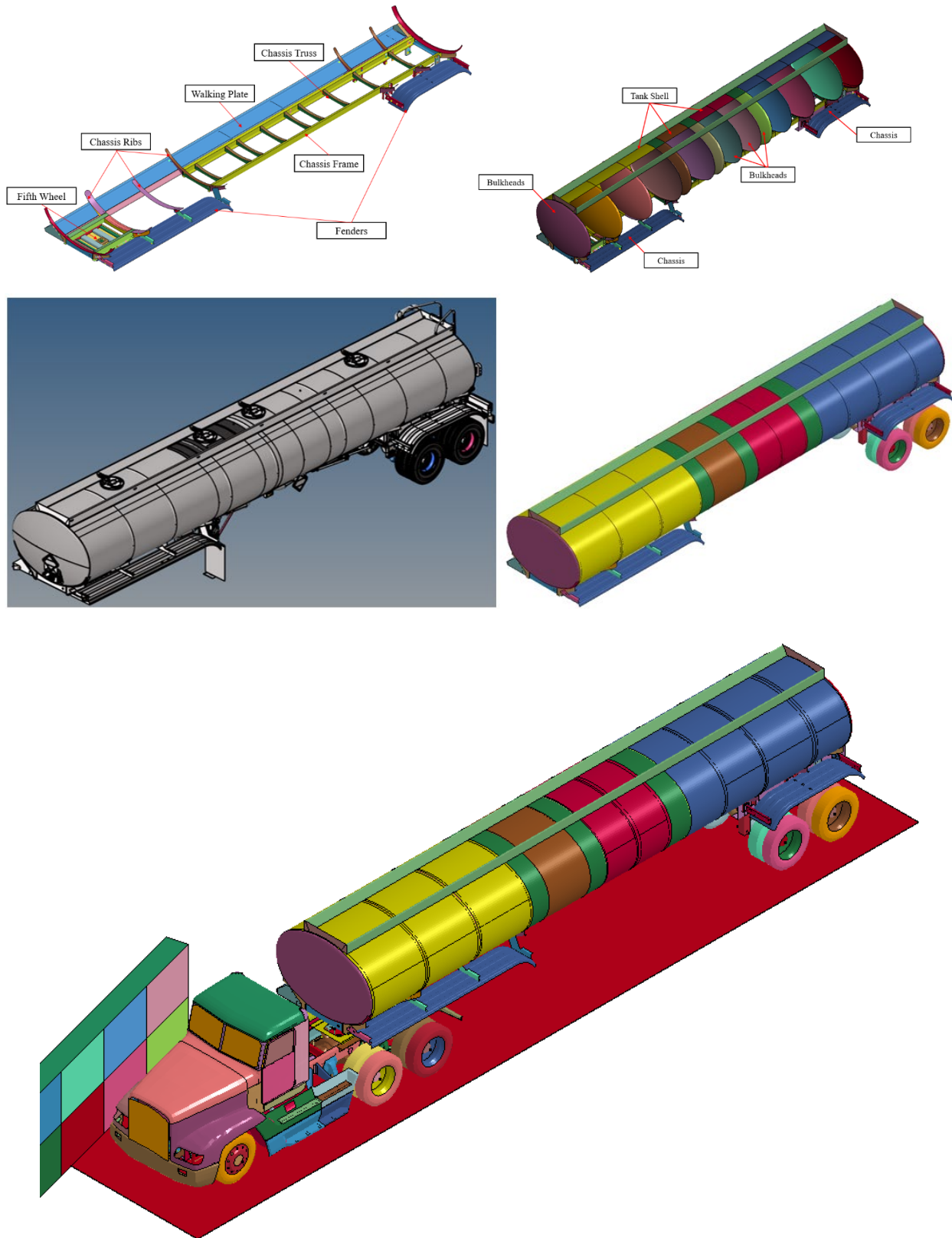
Figure 2.1 FEA Model of MASH 36,000T Tractor-Tank Trailer Vehicle

Using the tractor-tank trailer simulation model, a parametric study in LS-DYNA was performed on various barrier heights. The simulations included the 36000T vehicle impacting vertical, rigid barriers ranging in height between 50 and 90 in. under MASH TL-6 impact conditions (i.e., 50 mph and 15 degrees). Maximum roll angles for the tractor and trailer were measured for each simulation. Additionally, the impact loads imparted to the barrier were measured for each simulation.

TL-6 impact events may occur over significant periods of time. A typical MASH TL-3 vehicle impact into a rigid wall may result in the vehicle exiting the barrier 300 ms - 400 ms after impact, where the simulated 36000T tractor-tank trailer vehicle was in contact with the barrier 1,500 ms after impact. Unfortunately, the modeled fluid within the tank trailer often became unstable, forcing LS-DYNA simulations to terminate prematurely as the simulation continued past 1 second after impact. All of the simulations ran for at least 900 ms before terminating. Therefore, the simulation comparisons shown herein were taken within the first 900 ms of the impact event. Note, in most of the simulations, the vehicle had already reached its maximum roll by 900 ms.

As expected, the lower barrier heights produced higher vehicle roll angles during the impact event. A comparison of the vehicle positions at 900 ms after impact for a small sample of barrier heights is shown in Figure 2.2.

The maximum roll achieved by the vehicle in each simulation is shown graphically in Figure 2.3. The magnitude of vehicle roll steadily decreased as barrier height increased from 50 in. to 70 in. Note that the tank trailer had not stopped its roll motion in the simulations for barrier heights of 50 in. and 55 in. Above a barrier height of 70 in., each incremental increase in barrier height resulted in minimal reductions to the maximum roll angle.

50-in. Tall Barrier
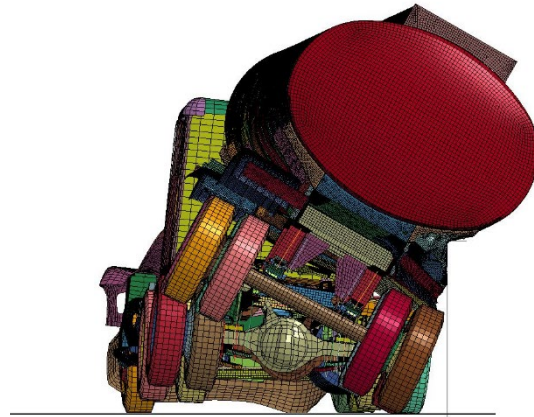


62-in. Tall Barrier



70-in. Tall Barrier



90-in. Tall Barrier

Figure 2.2 Comparison of Vehicle Positions at Time of Maximum Roll
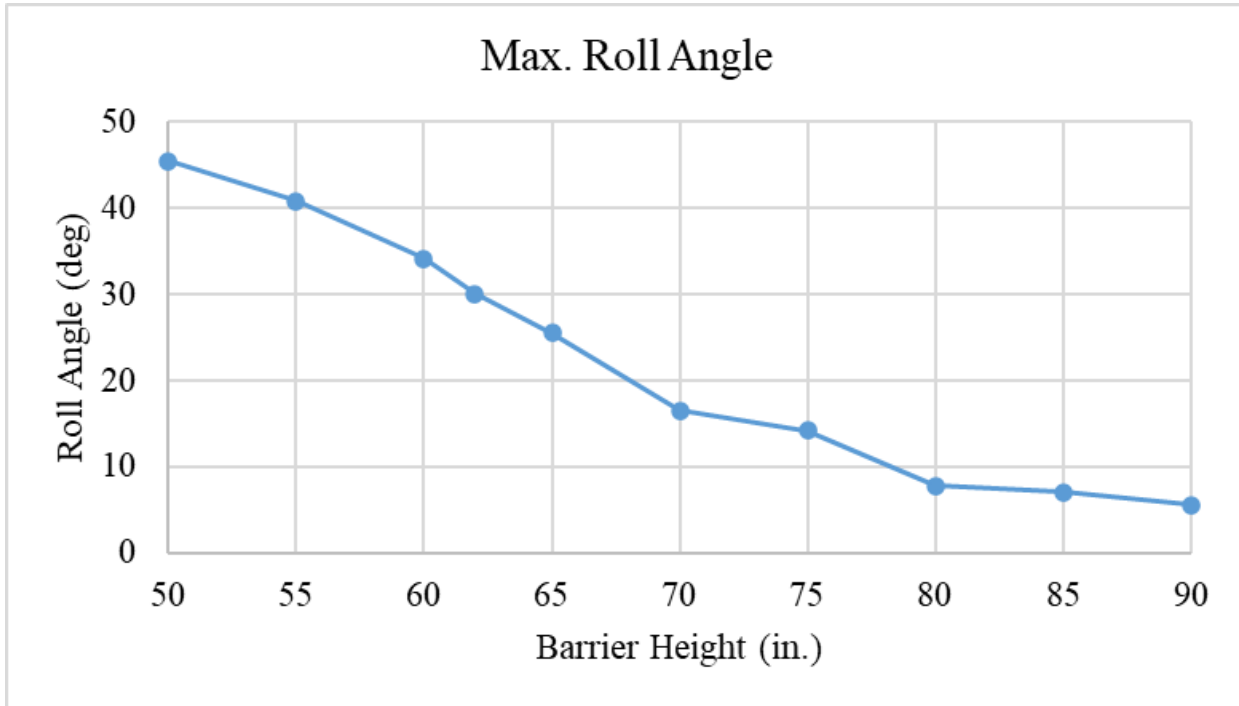
Figure 2.3 Maximum Vehicle Roll vs. Barrier Height

As described previously, simulations conducted on barrier heights less than 60 in. showed continued vehicle roll when the simulation prematurely terminated. Thus, there existed elevated risk for the vehicle to roll over the barrier (i.e., barrier override) at these low heights. Simulations with barrier heights ranging from 60 in. to 70 in. showed significant roll angles, but the vehicles stabilized and began to return to an upright position. However, there were concerns with roll angles above 30 degrees as the fluid in the tanks would slosh around and possibly result in vehicle instabilities. Therefore, the 62-in. tall barrier, which limited the roll angle to 30 degrees, was deemed a reasonable top height for capturing a MASH 36000T vehicle.

The shape of a concrete barrier can greatly affect the trajectory and stability of an impacting vehicle. Multiple studies have been conducted showing that vehicle stability is maximized for barriers with flat, vertical walls [21-23]. Accordingly, a vertical front face was considered ideal for the new high-performance barrier system.

Vertical barriers or walls cannot be easily slip formed, which is a process that can significantly reduce installation costs by eliminating traditional formwork construction. Most barrier installers using slip-formed construction prefer a sloped face (i.e., batter) greater than or equal to 12V:1H. Using a 12H:1V front slope, the top corner of a barrier measuring 62 in tall would be set back 5.2 in. away from the toe of the barrier. To create a round number and still satisfy the 12V:1H requirement, the top was set back 6 in. for the new TL-6 barrier system.

2.2 Design Loads

In a previous study, researchers conducted a full-scale crash test with a 79,900-lb tractor-tank trailer vehicle impacting an instrumented wall at a speed and angle of 54.8 mph and 16.0 degrees, respectively [19], which matches the impact conditions of MASH test designation no. 6-12. During the test, the maximum 50-ms average impact load measured by the instrumented wall was approximately 370 kips. However, the maximum 50-ms average impact load predicted by the LS-DYNA simulations, which were utilized to determine the critical barrier height, was around 300 kips. Therefore, the researcher team decided to be aggressive and utilize a 300-kip lateral design load for configuring the new TL-6 barrier system.

The simulated impacts with the TL-6 tractor-van trailer vehicle revealed two distinct load application heights. The tank applied high magnitude impact loads near the top of the simulated barriers, while the wheels applied significant load to the lower portion of the barrier. Further, the tank load applied at the top of the barrier accounted for about 2/3 of the total impact load. Therefore, the design loads for the new barrier were 200 kips applied at the top of the barrier and 100 kips applied at the height of the center of the rear tandem axle, which was estimated to be 22 in. The design loads are shown in Figure 2.4.

August 7, 2024

MwRSF Report No. **Error! Reference source not found.**
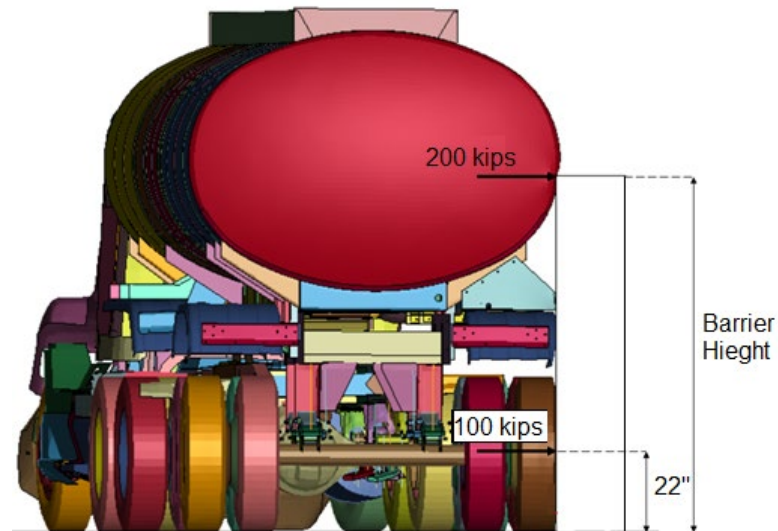
Figure 2.4 Barrier Design Loads

2.3 Barrier Design

      The TL-6 barrier's steel reinforcement and width were optimized for strength and installation costs. Efforts were made to limit barrier width and internal steel reinforcement in order to reduce installation costs. The barrier's strength was calculated using a modified Yield-Line analysis method. Instead of the typical V-shaped failure pattern assumed for barrier analysis in the AASHTO *LRFD Bridge Design Specifications* [24], a trapezoidal failure pattern presented, as presented by Jeon et al. [25], was used for calculating the strength of the barrier. This failure pattern is shown in Figure 2.5, and the equations for calculating barrier strength calculation are depicted as Equations 1 and 2 below:

$$L_c = L_t + \sqrt{\frac{8 M_w H_1}{M_{c,ave}}} \tag{1}$$

$$R_w = \left(\frac{H_1}{H_e}\right) \left[ M_{c,base}\left(\frac{L_t}{H_1}\right) + M_{c,avg}\left(\frac{L_c - L_t}{H_1}\right) + M_w\left(\frac{8}{L_c - L_t}\right) \right] \tag{2}$$

where   $L_c$ = critical length of the failure pattern
$L_t$ = length of the applied load
$H_1$ = height of the barrier
$H_e$ = effective height of the applied load
$M_w$ = moment capacity of the wall about a vertical plane
$M_{c,base}$ = overturning moment capacity at the base of the barrier
$M_{c,ave}$ = average overturning moment capacity of the barrier
$F_f$ = magnitude of the applied load
$R_w$ = strength capacity of the barrier
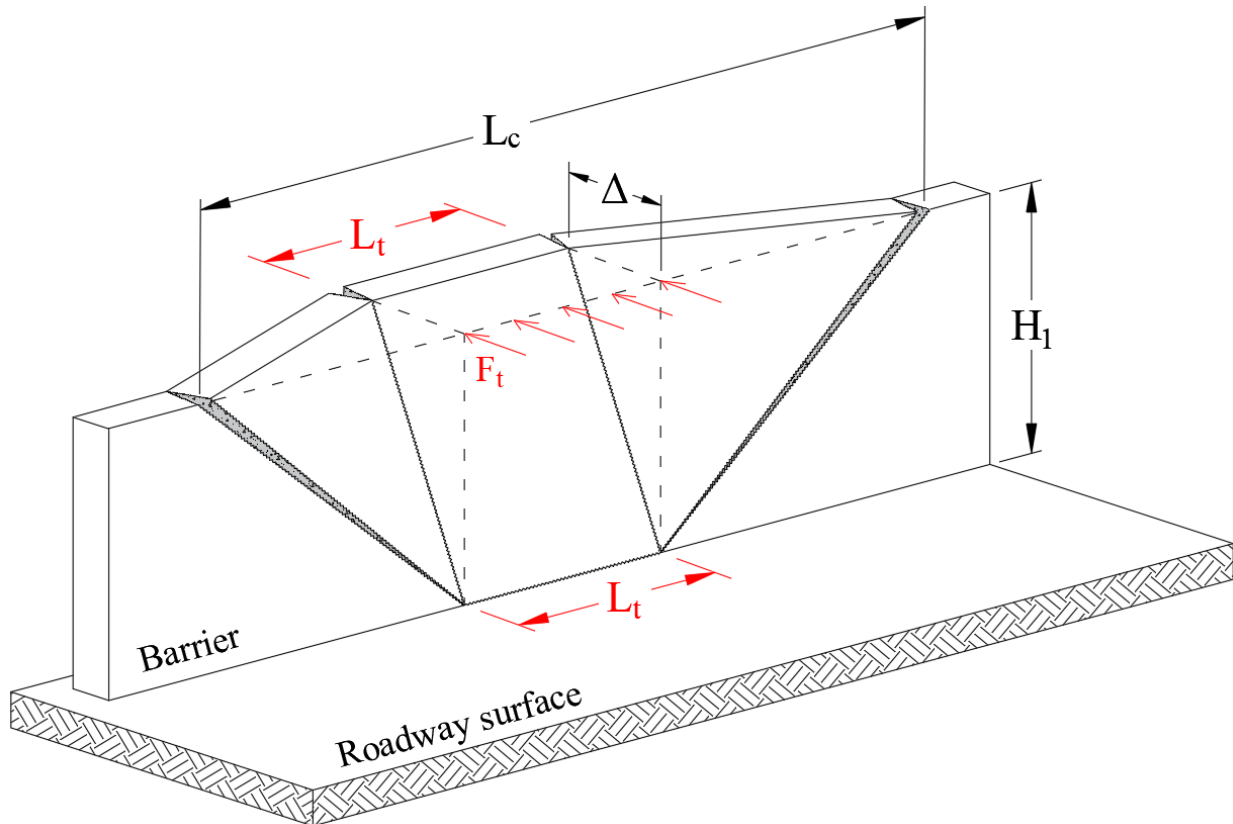


Figure 2.5 Trapezoidal Failure Pattern for Yield-Line Theory Analysis [25]

The length of the applied load, $L_t$, for a tractor-tank trailer was estimated to be 10 ft. Since the design loads were applied at two different heights, a weighted average was used to calculate an effective height of 48.7 in.

Multiple variations of longitudinal steel, transverse steel, and barrier width were analyzed until an optimized barrier configuration was selected. The selected barrier design is shown in Figure 2.6. The width of the barrier at the top and base were 10 in. and 22 in., respectively. The steel reinforcement for interior regions of the barrier consisted of 14 longitudinal no. 6 rebars in the section, seven bars on the front face and seven bars on the back face, along with no. 5 vertical stirrups spaced on 12 in. centers and anchored into a concrete foundation. The vertical stirrups were embedded 10 in. into an existing concrete tarmac measuring approximately 20 in. to 24 in. thick. The vertical stirrups were installed using an epoxy adhesive which allowed the full strength of the bars to be developed. A 2-in. concrete clear cover was used around all steel reinforcement. The final design was estimated to have a lateral resistive capacity of 313 kips. Steel reinforcement details were also developed for the end of the barrier or for regions where expansion  and contraction joints were desired. For exterior or end regions, the longitudinal steel reinforcement was identical to that used for interior regions, which was 14 no. 6 bars. However, the no. 5 vertical stirrups were reduced from a 12 in. to 5 in. spacing to maintain the necessary barrier capacity at discontinuities or ends. The end barrier length for the 5-in. vertical bar spacing was just under 15 ft.
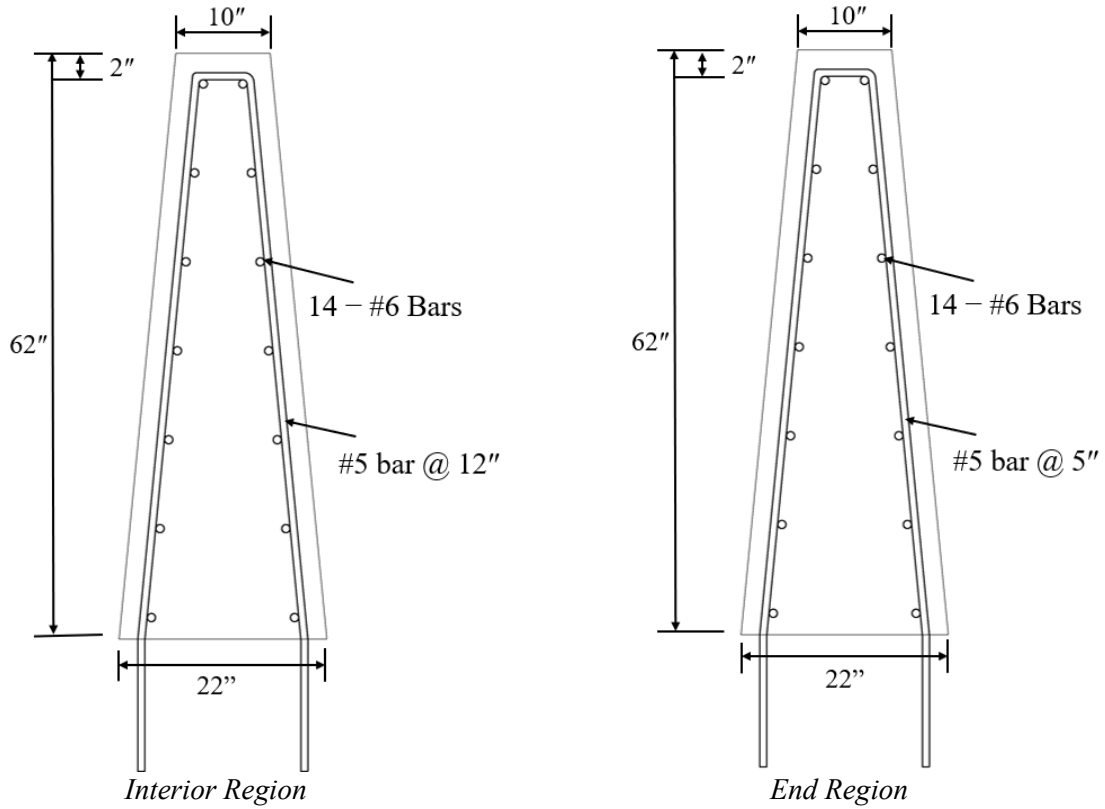
Figure 2.6 Interior and End Cross Sections for MASH TL-6 Concrete Barrier (Not to scale)

Chapter 3 Full-Scale Crash Test Overview – Test No. MTL6-1

3.1 Test Vehicle

The test vehicle (i.e., tractor) was acquired and consisted of a 2010 Freightliner Columbia with a curb weight of 26,814 lb, which was later prepared for the full-scale crash test. The tank trailer consisted of a 1997 LBT tank trailer model 4466 with a total tank capacity of 8,721 gallons. After ballasting, the test inertial weight of the complete TL-6 test vehicle was 79,884 lb. The complete test vehicle dimensions are shown in Figure 3.1. Additional trailer dimensions are provided in Figure 3.2.

The tank trailer consisted of four compartments isolated with bulkheads at each end, and interior baffle structures which both provided lateral stiffness for the outer jacket and reduced longitudinal sloshing of the fluid cargo. The sizes of the four compartments of the tank were 4,000 gal, 1,200 gal, 1,500 gal, and 2,800 gal (nominal), proceeding from the front of the tank to the rear. The heights of the fluids in each tank were 37 in., 59⅜ in., 46½ in., and 39½ in., respectively. A visual depiction of the fill heights of the tanks in the trailer is shown in Figure 3.3.

August 7, 2024

MwRSF Report No. **Error! Reference source not found.**



Figure 3.1 2010 Freightliner Columbia Truck Dimensions, Test No. MTL6-1

**Test Name:** MTL6

**Tractor:**

| Model Year: | 2010 | Make: | Freightliner | Model: | Columbia 112 | VIN No.: | 1FUJFOCV2ADAV1130 |

Odometer: 503917.9

**Trailer:**

| Model Year: | 1196 | Make: | Fruehauf Trailer Co. | Model: | Tanker Trailer | VIN No.: | 8VT 001601 |

**Vehicle Geometry - in. (mm)**
Target Ranges listed below

A: 94 3/4 — 2406 1
B: 108 3/4 — 2762
C: 701 — 17805  Max: 780 (19850)
D: 50 1/4 — 1276
E: 155 — 3937
F: 51 1/4 — 1301
G: 362 1/4 — 9201
H: 49 — 1244
I: 33 1/4 — 844 11/20  Max: 73 (1850)
J: #DIV/0! — #DIV/0!
K: 77 1/8 — 1958 39/40  81±4 (2050±100)
L: 63 1/4 — 1606 11/20
M: 31 1/4 — 793 3/4
N: 12 — 304 4/5
O: 2 — 50 4/5
P: 35 — 889
Q: 45 1/2 — 1155 7/10
R: 120 1/2 — 3060 7/10
S: 28 3/8 — 720 29/40
T: 39 1/2 — 1003 3/10
U: 84 1/8 — 2136 31/40
V: 75 5/8 — 1920 7/8
W: 73 1/4 — 1860 11/20
X: 98 — 2489 1/5
Y: 16 — 406 2/5
Z: 481 — 12217 2/5
AA: 75 3/4 — 1924 1/20
IW: 44 3/8 — 1127 1/8

**Weights - lb (kg)**

Tractor Wheel Base: 180 5/8 — 4587 7/8  Max: 200 (5100)

| | Curb | Test Inertial | Gross Static |
|---|---|---|---|
| M1: | 8562 — 3883 52/79 | 10145 — 4601 41/59 | 10200 — 4626 9/14 |
| M2: | 4760 — 2159 1/10 | 17544 — 7957 33/40 | 17598 — 7982 15/47 |
| M3: | 4412 — 2001 1/4 | 16625 — 7540 37/38 | 16678 — 7565 1/71 |
| M4: | 3220 — 1460 21/37 | 15300 — 6939 53/55 | 15300 — 6939 53/55 |
| M5: | 4660 — 2113 20/27 | 20250 — 9185 16/65 | 20250 — 9185 16/65 |
| Total: | 25614 — 11618 6/19 | 79864 — 36225 19/27 | 80026 — 36299 5/27 |
| | 29,000±3,100 (13,200±1,400) | 79,300±1,100 (36,000±500) | |

Longitudinal C.G.: 342 7/16 — 8697 73/80
Ballast Weight - lb (kg): 55110 18/25 — 24997 41/51

Vertical C.G. not measured or recorded
Wheel Center Height M1: 19 — 482 3/5
Wheel Center Height M2: 19 5/8 — 498 19/40
Wheel Center Height M3: 19 5/8 — 498 19/40
Wheel Center Height M4: 20 — 508
Wheel Center Height M5: 19 1/2 — 495 3/10

**Surrogate Occupant Data**

Type: Hybrid II
Mass: 161 lb
Seat Position: Left/Driver

Engine Type: Diesel
Engine Size: 12.8L I6
Transmission Type: Manual
Drive Type: RWD

Note any damage prior to test: No significant damage, scrapes, dings only.

BKZ 4466

**ESTIMATED WEIGHT SUMMARY**

| | | |
|---|---|---|
| Payload | 8721 Gals. @ 6.1 #/Gal. | 53200# |
| Tank | 5640# | |
| Chassis | 4660# | *Trailer 10300 |
| Tractor | | 16500 |
| Total | | 80000# |

*Trailer weight does not include any customer added equipment such as hoses, fittings, etc.

89.1% Shell Full
Max. load 57000#
GVWR 68000#
GAWR 20000#

MODEL TAG-F2-ESF 9500 X 4DB  Sheet 1 of 7
CONSTRUCTION ALUMINUM  (96" WIDTH)

THIS UNIT IS ENGINEERED AND CONSTRUCTED OF MATERIALS SHOWN TO HAUL THE COMMODITIES INDICATED AND IS INTENDED FOR OPERATION AT REASONABLE SPEEDS UNDER NORMAL ROAD CONDITIONS. LBT, INC. OR THE FRUEHAUF TRAILER CORPORATION ASSUMES NO RESPONSIBILITY FOR:
1. WEIGHTS OR CAPACITY OF TRACTOR.
2. OVERLOADS OR DAMAGE IF COMMODITY WEIGHTS EXCEED THOSE SHOWN OR MODEL RATING.
3. DAMAGE CAUSED BY COMMODITIES, CLEANING, OR OPERATION NOT COMPATIBLE WITH MATERIALS OF CONSTRUCTION SPECIFIED.
SEE ATTACHED SHEET FOR SPECIFICATIONS.

56'- 0 1/2" Overall Tractor-Trailer Length
42'- 6" Approx. Overall Trailer Length

112"   58"   ₵ KINGPIN   478 1/2" Seam-to-Seam ( 479" Tank Proper )   24"

TRACTOR
All Dimensions & Weights Assumed.

28 1/2"   ₵ TANDEM   417"   33"
21 1/2"   C.G. Tank & Load   TANDEM ₵
211 3/4"   58840#
186"   15"   50 3/4"   15"   65 1/4"   18 1/2"   128"

4000 Gals.   1200 Gals.   1500 Gals.   2800 Gals.

APPROX. 129 1/2" O.A.H.

49"

₵ SUPPORTS

108" C.A.   25"   24 1/2" 24 1/2"
28"   192" W.B.   395 1/2"   57"

| | | |
|---|---|---|
| 8700# | Tractor | 7800# |
| 3300 | Coupler Load | 26200 |
| 12000# | Total | 34000# |

| | | |
|---|---|---|
| Chassis | 4100# |
| Tank & Load | 29900 |
| Total | 34000# |

37'- 1"
51'- 0"

NOTE: DRAWING NOT TO SCALE   REF: BKZ 4226   OPERATION NATIONAL NETWORK

LBT Inc.
P.O. BOX 24209
OMAHA, NE 68124-0209
T: (402) 333-4900
F: (402) 333-0685

CUSTOMER SEMI-SERVICE, INC.
DEALER/BRANCH #743
COMMODITY GASOLINE, FUEL OIL
CAPACITY 9500 GALS + 3%   8VT 001601
DATE 06-19-96 BY S. HEVELONE   BKZ 4466

LET.   REVISIONS   ENG.   DATE

Figure 3.2 1997 LBT 4466 Tested Trailer Dimensions, Test No. MTL6-1
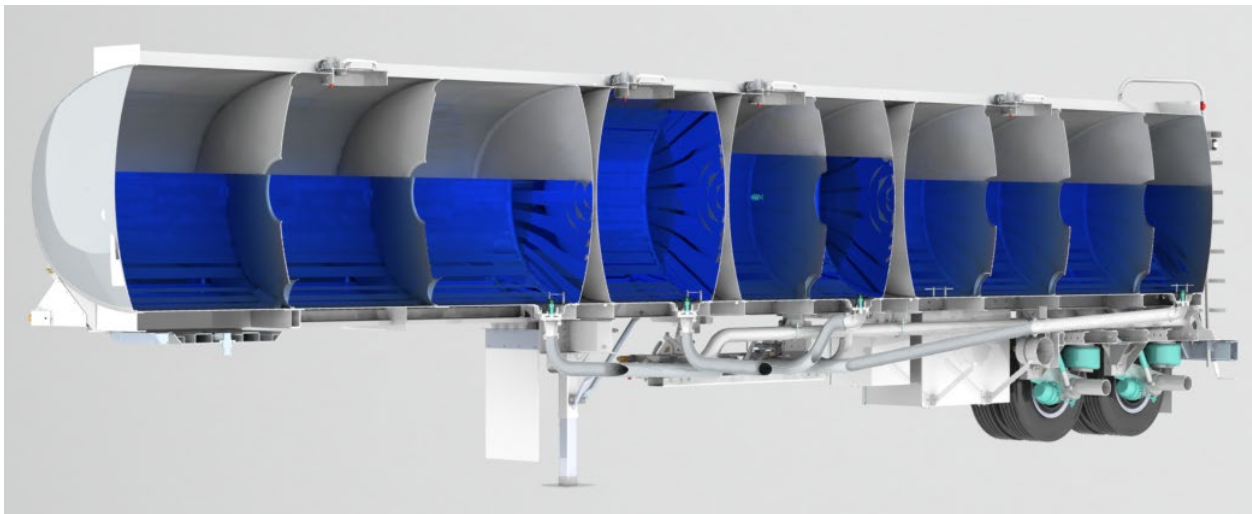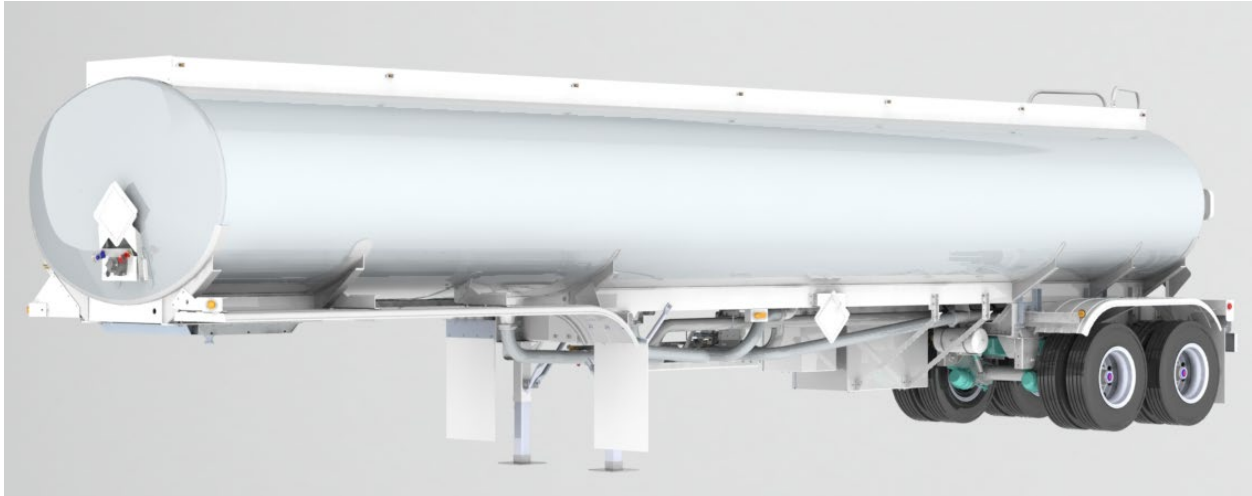
NOTE: Ballast shown with actual heights, but tested trailer model is slightly different than shown

Figure 3.3 Ballast Fill Distribution and To-Scale Fill Heights, Test No. MTL6-1

3.2 Test Article Design Details

The test installation for the TL-6 barrier was 187 ft - 6 in. long. The reinforced concrete barrier was 62-in. tall and had a 5.5-degree single-slope (i.e., constant slope) face on the front and back sides, as shown in Figure 3.4. The barrier had a 22 in. base width and a 10-in. top width. A ¾-in. wide expansion joint was placed in the barrier approximately 37 ft - 6 in. away from the upstream end of the test installation. No load transfer mechanisms were included across the barrier joint. End section reinforcement consisted of the 5-in. vertical stirrup spacing over a length of 14.3 ft on both sides of the open joint. The concrete had a minimum compressive strength of 5,000 psi.

The barrier was reinforced with 14 no. 6 longitudinal bars – seven bars on front face and seven on the back face. Vertical stirrup reinforcement consisted of no. 5 bars embedded into the concrete tarmac to a depth of 10 in. using Hilti HIT-RE 500 V3 epoxy anchor adhesive. The vertical reinforcing bars were spaced 5 in. apart at end sections and 12 in. apart at interior sections. All steel rebar had a minimum yield strength of 60 ksi. A 2-in. concrete clear cover was used around all steel reinforcement.

(a) Interior Section



(b) End Section



(c) TL-6 Concrete Barrier System

Figure 3.4 MASH TL-6 Single-Slope Concrete Barrier System, Test No. MTL6-1

3.3 Test No. MTL6-1

Test No. MTL6-1 was conducted on the new TL-6 barrier according to the impact conditions of MASH test designation no. 6-12, which consists of a 36000T tractor-tank trailer vehicle weighing 36,000-kg (79,366-lb) impacting at a target speed and angle of 50 mph and 15 degrees, respectively. MASH test designation no. 6-12 is intended to evaluate the strength of the barrier for containing and redirecting heavy trucks. Additional evaluation criteria beyond containing and redirecting the impact vehicle include meeting limits for occupant compartment integrity and providing adequate vehicle stability. For vehicle stability, MASH TL-6 does not require that the truck remain upright during and after the collision as the primary purpose of the test is to demonstrate that the barrier can contain and redirect the vehicle. However, MASH does denote that the vehicle is limited to a one-quarter roll.

The critical impact point for test no. MTL6-1 was selected to impact the front corner of the tractor-tank trailer vehicle at the centerline of the expansion joint or 450 in. downstream from the upstream end of the barrier. The impact point was selected using LS-DYNA analysis to maximize loading near the expansion joint of the barrier due to impact of the rear tandem axles of the tank trailer upstream from the joint. Impact of the tandem axles just upstream from the expansion joint maximized lateral loading to the barrier at the critical discontinuity (i.e., expansion joint). This approach ensured proper evaluation of barrier capacity at a barrier end region, which was configured with slightly less lateral capacity than interior regions. The impact point was also selected to increase the potential for snag of the tank trailer on any exposed surfaces near the expansion joint.

During test no. MTL6-1, the 80,026-lb (79,864-lb test inertial) tractor-tank trailer impacted the centerline of the barrier's expansion joint at a speed of 51.1 mph and at an angle of 15.7 degrees. Immediately following the initial impact, the tractor portion of the vehicle began to

be redirected by the barrier. By 0.280 sec after impact, the tractor section of the vehicle had become parallel with the barrier, and the leading edge of the tank trailer had impacted the top of the parapet. As the tractor-tank trailer vehicle continued to be redirected, the lower third of the tanker was supported by the top of the concrete parapet as the tractor-tank trailer vehicle rolled towards the barrier. By 0.680 sec after impact, the tank trailer had become parallel with the barrier. By 2.150 sec after impact, the tractor-tank trailer vehicle had exited the barrier, continued downstream, and rolled back away from the barrier. The vehicle continued downstream, and the roll motion of the tractor-tank trailer vehicle continued due to a combination of vehicle momentum as it exited the barrier and the sloshing of the fluid ballast inside the tank trailer. The roll motion continued until the tractor-tank trailer vehicle rolled onto its right side at approximately 3.7 sec after impact. After rolling onto its right side, the tractor-tank trailer vehicle proceeded to slide downstream on its right side for approximately 2.8 seconds. At approximately 6.5 sec after initial impact, additional roll motion was induced into the vehicle likely due to a combination of several factors. The increased roll motion occurred from the momentum of the sliding vehicle with fluid sloshing in the tank trailer, the vehicle's orientation already being on its right side, and the uneven surface features on the test site's concrete tarmac (i.e., uneven cut joints over time), combined to induce approximately 180 degrees of additional roll after previously sliding on its side. The vehicle came to rest on its left side. This additional roll caused significant crush deformations to the tractor's cab. The tractor-tank trailer vehicle came to rest 310 ft downstream from the initial impact location. A summary of the test events is shown in Figure 3.5. Sequential images of the test are shown in Figure 3.6.

Vehicle and barrier damage are shown in Figure 3.7. Damage to the barrier was minimal and consisted of contact marks, scrapes, gouging, fracture of concrete at the traffic side face of the upstream and downstream edges of the expansion gap, and chipping at the top, traffic-side

edge of the barrier in the contact region. No significant structural damage was noted on the barrier, and no measurable dynamic or permanent set barrier deflections were observed. The total length of vehicle contact was 90 ft - 6 in.

Damage to the vehicle was extensive, which was primarily due to the sliding and secondary rollover events after exiting the barrier system, as shown in Figure 3.7. The cab, windshield, roof, and both side doors were crushed inward. The cab frame experienced tears, which caused the roof and door structures to collapse inward as the vehicle lifted to an upright position after the test. Scraping, minor gouging, and some peeling of the aluminum jacket were observed near locations of trailer baffles. The left side of the tank trailer had two small holes due to contact and grinding along the top of the parapet. The right side of the trailer experienced extensive scraping in the diagonal, mostly vertical direction corresponding to sliding on the concrete tarmac, with multiple small tears and holes observed in the aluminum jacket, especially near the internal baffles or end walls. The right side was flattened and crushed inward along the entire middle section, where the vehicle rolled and skidded. Several tears were observed in the jacket measuring between 2 and 3 in. long. One tear was observed in the undercarriage of the tank. Review of the tank trailer also found that the lids and seals along the top surface were leaking due to damage from the impact sequence, including subsequent rollover.

| 0.000 sec | 0.200 sec | 0.400 sec | 0.600 sec | 0.800 sec |
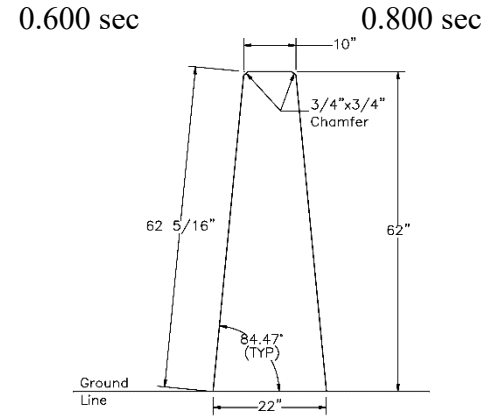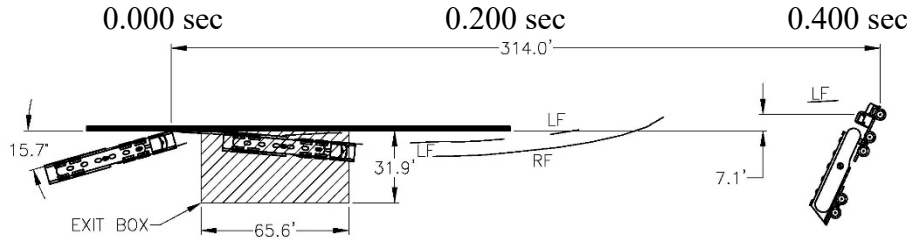




- Test Agency ................................................................................MwRSF
- Test Number.................................................................................. MTL6-1
- Date.................................................................................................12/8/2021
- MASH Test Designation No. ...........................................................6-12
- Test Article.......................................... MASH TL-6 Concrete Barrier
- Total Length ...........................................................................187 ft – 6 in.
- Key Component – Concrete Barrier
  Length ..............................................................................187 ft – 6 in.
  Height.......................................................... 62 in. from top of tarmac
- Soil Type.............................................. Coarse, crushed limestone (well-graded gravel)
- Vehicle Make /Model.............. Freightliner Columbia 112 with Fruehauf Tanker Trailer
  Curb ..........................................................................................25,614 lb
  Test Inertial....................................79,864 lb (MASH 2016 Limit 79,300 ± 1,100 lb)
  Gross Static....................................................................... 80,026 lb
- Impact Conditions
  Speed .........................................................51.1 mph (MASH Limit 50 ± 2.5 mph)
  Angle .......................................................... 15.7 deg (MASH Limit 15 ± 1.5 deg)
  Impact Location................ 450 in. downstream from the upstream end of the barrier
- Impact Severity ............................................510.5 kip-ft > 404 kip-ft MASH 2016 limit
- Exit Conditions
  Speed ..............................................................................................36.5 mph
  Angle ...............................................................5 deg (approximately)
- Exit Box Criterion .......................................................................N/A
- Vehicle Stability..............................................................................
- Vehicle Stopping Distance ................................310 ft downstream, 14 ft laterally behind
- Vehicle Damage................................................................................ Severe
  VDS ....................................................................................................N/A
  CDC.....................................................................................................N/A
  Maximum Interior Deformation .................................................................N/A

- Test Article Damage .................................................................................Minimal
- Maximum Test Article Deflections
  Permanent Set.................................................................................... N/A
  Dynamic ............................................................................................0.4 in.
  Working Width.................................................................................. 37.2 in.
- Transducer Data

| Evaluation Criteria | | Transducer | | | MASH Limits |
|---|---|---|---|---|---|
| | | SLICE-1 (in cab) | SLICE-2 (rear axle) | TDS (truck rear) | |
| OIV ft/s | Longitudinal | -3.36 | -4.44 | 16.21 | not required |
| | Lateral | 13.70 | 4.71 | 24.90 | |
| ORA g's | Longitudinal | 3.67 | -5.00 | 43.37 | |
| | Lateral | 7.36 | 15.73 | 28.08 | |
| Maximum Angular Displacement deg. | Roll | 265.2 | 276.0 | - | ¼ roll |
| | Pitch | 11.12 | 2.15 | - | not required |
| | Yaw | 33.57 | -29.38 | - | |
| THIV – ft/s | | 35.18 | 20.46 | - | not required |
| PHD – g's | | 7.36 | 16.01 | - | |
| ASI | | 0.71 | 1.21 | 2.58 | |

Figure 3.5 Summary of Test Results and Sequential Photographs, Test No. MTL6-1

30

August 7, 2024
MwRSF Report No. **Error! Reference source not found.**

| | | |
|---|---|---|
| 0.000 sec | 0.600 sec | 2.100 sec |
| 0.100 sec | 0.700 sec | 3.100 sec |
| 0.200 sec | 0.800 sec | 4.100 sec |
| 0.300 sec | 0.900 sec | 5.100 sec |
| 0.400 sec | 1.000 sec | 6.100 sec |
| 0.500 sec | 1.100 sec | 8.100 sec |

Figure 3.6 Sequential Images, Test No. MTL6-1

Figure 3.7 System and Vehicle Damage, Test No. MTL6-1

Test results indicated that the vehicle was contained and redirected, but the momentum of the vehicle roll of the tank trailer and lateral movement of the fluid ballast caused the vehicle to roll 90 degrees onto the right side after exiting the barrier. Subsequently, while sliding to a stop, the rocking motion of the fluid in the interior tanks, the vehicle orientation on its side, and potential uneven surfaces on the test site tarmac contributed to a secondary 180-degree rollover event near the point of final rest. The rotational motion of the tractor and tanker trailer during the impact are shown in Figure 3.8. Review of the tractor-tank trailer vehicle roll motion shows that the initial rollover of the vehicle onto its right side was consistent with the roll of the vehicle as it exited the barrier. After the tractor-tank trailer vehicle rolled onto its right side, the vehicle slid downstream on its side for approximately 2.8 sec for a total of 6.5 sec prior to the final rollover. This relatively long period of stable vehicle translation downstream may suggest that several factors, such as fluid sloshing and uneven tarmac surfaces, may have led to the secondary roll motion, as mentioned previously.
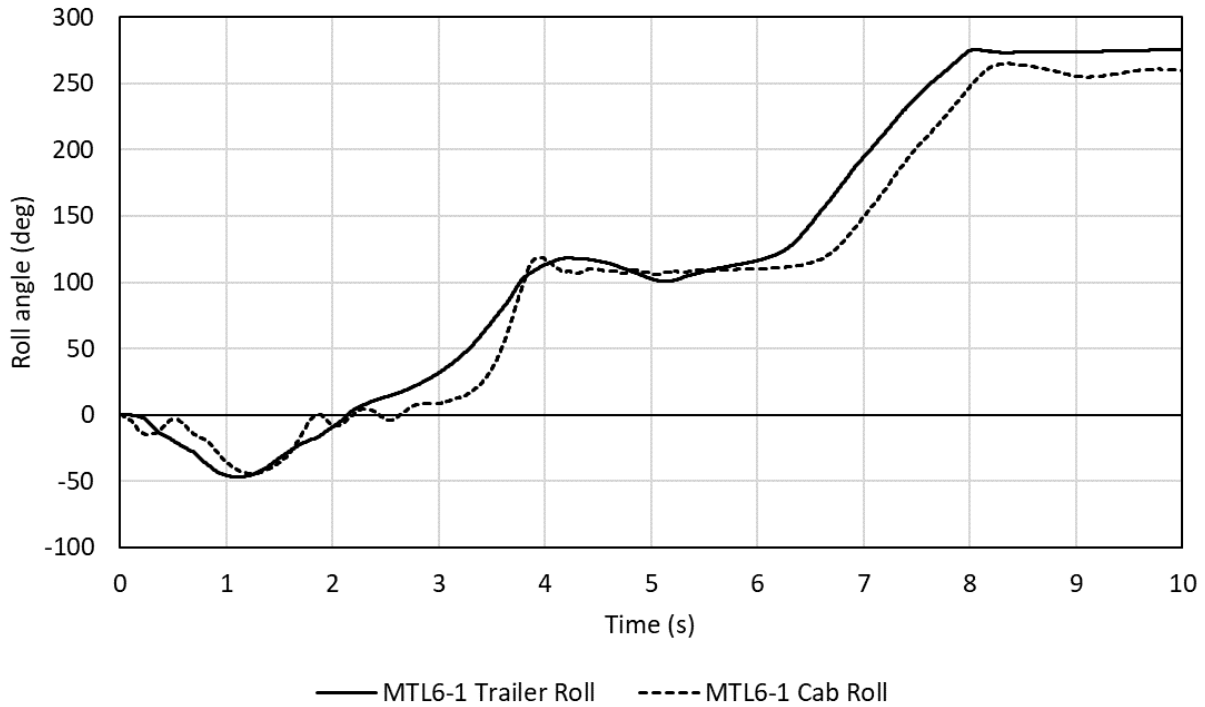
Figure 3.8 Vehicle Roll Angles, Test No. MTL6-1

The analysis of the test results for test no. MTL6 1 showed that the system contained and redirected the tractor-tank trailer vehicle with controlled lateral displacements of the barrier, but the vehicle did not remain upright following the initial impact event. Deformations of, or intrusions into, the occupant compartment that exceeded MASH limits and could have caused serious injury occurred during the secondary rollover event at the conclusion of the vehicle's post-impact trajectory. As noted previously, MASH criteria for test designation no. 6-12 permits a vehicle to roll onto its side but not exceed one-quarter turn. Thus, the vehicle trajectory and deformation of the tractor's occupant compartment during the second rollover event would suggest that the TL-6 barrier system did not meet all of the criteria for test designation no. 6-12.

However, the primary research objective included the development of a MASH TL-6 barrier system to contain and redirect tractor-tank trailer vehicles under extreme impact conditions, thus preventing catastrophic outcomes resulting from barrier override or penetration

through barriers. This expectation existed for crash events occurring on the national and local

roadway network, including freeways, interstates, tollways, and highways. It was not imperative

that the tractor-tank trailer vehicle remain upright during the impact sequence. Further, it was

acceptable for the tractor-tank trailer vehicle to roll onto its side. As such, it was believed that the

crash-tested and evaluated concrete barrier system successfully met the primary objective to

contain and redirect MASH TL-6 tractor-tank vehicles.

Chapter 4 R&D Project Discussion, Summary, Conclusions, and Recommendations

Vehicle models were developed and calibrated as best as reasonably possible for simulating tractor-tank trailer vehicle crashes into tall, high-performance, barrier systems. Simulation results were used to select a reduced-height barrier for containing and redirecting tractor-van trailer vehicles under high-energy impact events under MASH TL-6 impact conditions.

A 62-in. tall, concrete barrier system was configured using yield-line analysis procedures and a 300-kip design lateral load, 200 kips at the top and 100 kips at center wheel location. The 187.5-ft long barrier system incorporated top and bottom widths of 10 in. and 22 in., respectively, and utilized a ¾-in. wide expansion gap downstream from the upstream end.

One crash test was performed on the barrier system using a Columbia 112 Freightliner and LBT tank trailer with a gross static weight of 80,026 lb, a test inertial weight of 79,864 lb, and impacting at 51.1 mph and 15.7 degrees under MASH test designation no. 6-12. The barrier successfully contained and redirected the tractor-tank trailer without barrier penetration and override. Minimal damage occurred to the reinforced-concrete barrier system.

Upon exit, the vehicle eventually rolled 90 degrees and slid on the concrete tarmac through 6.5 sec. The vehicle, including an oval-shaped tank with sloshing liquid cargo, traversed across the existing concrete tarmac with raised edges at the joints and began to roll another 180 degrees, whereby crush occurred to the truck's cab. During the impact event with the concrete barrier, two small holes were created in the left side of tank. During the impact event with the concrete ground, several holes were worn into the right side of the tank. Further, some of the relatively-new, upper tank hatches and seals were found to be leaking liquid cargo after the vehicle rotated 270 degrees and was laying on its side. Through 6.5 sec, the MASH TL-6 barrier

system contained and redirected the heavy vehicle with roll onto its side and with all occupant risk criteria met.

Note that the crash test described herein successfully demonstrated that a barrier system with a top height much lower than 90 in. would contain and redirect tractor-tank trailer vehicles under MASH TL-6 impact conditions. Crash tests with 1100C small cars (test designation no. 6-10) and 2270P pickup trucks (test designation no. 6-11) were deemed unnecessary due to prior successful crash tests on tall, vertical-shape, concrete barriers [26]. As a result, the new, optimized, 62-in. tall, reinforced-concrete barrier system was deemed crashworthy under MASH criteria for passenger vehicles. Further, the barrier system can be used in roadside, median, and bridge applications where mitigation of catastrophic risks associated with tractor-tank trailer vehicle crashes is desired.

In the prior-reported research findings [20], computer simulations had demonstrated that the vehicle's maximum roll angle was reduced from 30 deg to approximately 17 deg with a barrier height increase from 62 in. to 70 in. For situations where it is desirable to reduce the vehicle's risk of roll onto its side, the barrier could reasonably be constructed with 70-in. top height and a 5.5-degree slope away from vertical without the need for additional crash testing.

Finally, further discussions within the roadside safety community are recommended to determine proper crash test expectations for MASH TL-6 barriers subjected to high-energy impact events with round- or oval-shaped, tank-trailers.

Chapter 5 MASH TL-6 Considerations and Future Research

Full-scale crash testing of the new, TL-6 median barrier resulted in  the successful containment and redirection of the tractor-tank trailer vehicle, including vehicle stability for over 6.5 sec after initial impact with the barrier. However, a secondary rollover event described previously prevented the barrier system from being fully accepted as MASH crashworthy. The test outcome along with the limited number of existing TL-6 crash tests led to several potential considerations relative to conducting MASH TL-6 crash testing and evaluation efforts. First, MASH currently requires that tractor-tank trailer vehicles be ballasted through even distribution of the fluid ballast within the tanks in order to meet the target center of gravity height for the tank trailer. However, tank trailer designs have been lowered in height in recent years to improve stability. Thus, the research team had to fill ballast tanks unevenly to meet the minimum center of gravity height for the test described herein. As such, consideration of modified tank ballast guidance or revision of the ballast center of gravity height may be needed in the future.

Second, the one-quarter roll limitation for heavy vehicles may warrant further consideration with respect to tractor-tank trailer vehicles. The two previous TL-6 crash tests were conducted on extremely tall barrier systems, and the potential for tank trailer roll upon barrier exit was limited. Tractor-tank trailer vehicles also have an increased potential for roll due to their hard, round side profiles and sloshing fluid ballast. Thus, rollover criteria for tractor-tank trailer vehicles may require reconsideration as compared to the 10000S and 36000V vehicles in MASH, which have flat sides and rigidly anchored ballast, especially when considering shorter barrier heights.

Third, recommendations for heavy-vehicle runout areas may need reconsideration if vehicle stability is critical to the evaluation of a barrier system. Currently, many crash tests of heavy vehicles are conducted with clear runout areas that are relatively short after the test vehicle

exits the barrier. Thus, it is not uncommon for a vehicle to be directed into earth berms or other barriers shortly after exiting the barrier to prevent uncontrolled progress of the vehicle throughout a test site. The use shorter clear runout areas may prevent or limit the potential for the long-duration, secondary rollover event observed in the MASH TL-6 crash testing program described herein. A general review of previous crash testing programs has revealed that vehicle interaction with downstream barriers or terrain had been noted as the cause of a secondary rollover event that was deemed separate from the primary barrier impact event and did not adversely affect the evaluation of the barrier system. These statements may suggest that the configuration and length of the clear runout area may have significantly affected the rollover observed herein, and thus, further discussion of clear runout areas for heavy vehicle tests may be warranted within the roadside safety community. Finally, the primary objective for TL-6 barriers is containment and redirection of tractor-tank trailer vehicles. As vehicle rollover propensity may be increased for tractor-tank trailer vehicles, it may be worthwhile to reconsider expectations for using the occupant compartment crush evaluation criteria for MASH TL-6 heavy-truck crash tests.

Following the development and evaluation of the new MASH TL-6 concrete barrier, there existed a few other research needs. First, the TL-6 concrete barrier was installed as a standalone system that was anchored into an existing concrete tarmac. Real-world barrier installations will require (1) dedicated anchorage and foundation systems to accommodate the loads associated with potential impacts into this barrier and (2) geometric height transition designs to connect the new TL-6 concrete barrier to existing concrete barriers and guardrail systems. Suggestions for these features have been provided in the following chapter.

Second, the tractor-tank trailer vehicle simulation model that was developed in this research effort proved highly beneficial to determining the barrier height and geometry.

However, there were several areas for improvements to be made to the vehicle model, including refinement of the tank structure and connections, refinement of the tractor-tank trailer suspension, improvement of the fifth wheel connection, updates to the tank material models, and improved fluid and baffle structure modeling.

Finally, review of the damage to the tractor-tank trailer in the full-scale crash test noted holes in both sides of the tank structure due to contact with the barrier and the concrete tarmac, including leaking of newly-installed tank lids seals. As tractor-tank trailers are often tasked with transporting hazardous materials, it may be desirable to further study the damage observed in this crash test and conduct further research into improving the structural integrity and reinforcement of the tank to prevent dangerous spilling of their contents.

Chapter 6 TL-6 Barrier Implementation

6.1 Introduction

As previously discussed, the primary research objective was to develop a new MASH TL-6 barrier system to contain and redirect tractor-tank trailer vehicles. Even though this primary objective was achieved with the vehicle sliding on its side for 6.5 sec, the vehicle later experienced an additional roll scenario and another 180 deg of motion for a total of approximately 270 deg. This subsequent event caused significant crush of the tractor's cab, which may not be desired by some end users. However, some road authorities may have a strong desire to eliminate the risk of catastrophic crashes resulting from tractor-tank trailer vehicles penetrating through under-designed barriers or traveling over barriers with insufficient height. For these situations and understanding the risks noted above, the implementation of the new 62-in. tall, single-slope, concrete barrier may provide an economical option.

It is necessary to provide some general information to assist with its implementation in real-world applications. As already noted, the new barrier system should be adaptable for use in roadside, median, and bridge deck applications, as well as terminate in a manner that allows for its connection to common, crashworthy, approach guardrail transitions at its ends.

The development, testing, and evaluation effort was successful with the concrete barrier being anchored to an existing, 20-in. to 24-in. thick, non-reinforced concrete tarmac. The anchorage system included vertical stirrups that were embedded 10 in. into the concrete using a chemical, epoxy-adhesive material to develop the strength of the steel reinforcing bars. Again, this anchorage and foundation system was proven to be structurally adequate. However, alternative anchorage and foundation systems should also be deemed structurally adequate and not require further crash testing as long as they can reasonably provide equal or greater capacity and are conservatively configured.

6.2 Recent Barrier Anchorage Studies

Before configuring alternative anchorage and foundation systems, it was beneficial to briefly review several high-performance, crashworthy, concrete barrier systems. These studies were used to provide design knowledge pertaining to successful anchorage and foundation systems for high-performance barrier systems.

*6.2.1 TL-4 Shallow Anchorage for Single-Slope Traffic Rail (SSTR)*

In 2020, researchers at the Texas A&M Transportation Institute successfully crash tested and evaluated the MASH TL-4 single-slope traffic rail (SSTR) when attached to a shallow slab foundation system [27]. The general foundation consisted of a 4-in. thick, precast, reinforced-concrete panel embedded in and supported by the soil. The top of the 10-ft wide, precast panel was 4½ in. below grade. Another reinforced-concrete slab was cast on top of the precast panel and measured 4½ in. thick by 10 ft wide. The 36-in. tall SSTR was installed using cast-in-place construction and was vertically supported by the cast-in-place slab and precast panels. However, it was anchored using no. 4 vertical rebars that were only embedded within the 4½-in. thick, cast-in-place slab. The roadside edge of the concrete slab was attached to the roadway slab using no. 5 rebar dowels spaced on 24 in. centers.

*6.2.2 MASH TL-5 Single-Slope Concrete Barrier on Structurally Independent Foundations*

In 2019, researchers at the Texas A&M Transportation Institute successfully developed, simulated, crash tested, and evaluated the MASH TL-5 single-slope concrete barrier (SSCB) when attached to three foundation systems – shallow moment slab, vertical wall or grade beam, and drilled shaft foundations [28]. The three foundation options were optimized using computer simulation. The final systems included: (1) discrete 18-in. diameter by 6-ft deep, drilled, reinforced-concrete shaft foundations spaced on 11 ft centers at interior regions and 6 ft centers at gaps; (2) a continuous, 19-in. wide by 33-in. tall, reinforced-concrete, vertical wall or grade

beam foundation; and (3) a 10-ft wide by 18-in. thick, reinforced concrete moment slab foundation. Steel reinforcing bars connected the cast-in-place barrier to the reinforced-concrete foundation systems. Subsequently, the foundation system that exhibited the greatest deflection (i.e., drilled shaft foundations) was selected for the TL-5 full-scale crash testing program with the tractor-van trailer vehicle. The SSCB placed on discrete drilled shaft foundations successfully met the TL-5 crashworthiness criteria. Although only one of three foundation systems were subjected to full-scale crash testing and evaluated, the shallow moment slab and vertical wall foundation systems were also expected to meet the TL-5 impact performance criteria.

## 6.3 Roadside and Median Barrier Applications

For implementation of the MASH TL-6 single-slope concrete barrier in roadside and median applications, two general concepts for anchorage and foundation systems have been conservatively configured. For each scenario, the vertical stirrup bars would be anchored into the two types of anchorage and foundation systems – (1) a reinforced-concrete slab embedded in soil and (2) a reinforced-concrete grade beam embedded in soil.

For the concrete slab option, a conservative configuration consisted of a 12-in. thick by 12-ft wide reinforced-concrete foundation for interior sections, as shown in Figure 6.1. The concrete slab was strengthened using no. 6 transverse, steel reinforcing bars spaced on 6 in. centers in both the top and bottom mats. The longitudinal reinforcement consisted of 26 no. 6 steel bars – 13 in the top mat and 13 in the bottom mat. Concrete slab options for end regions have not been configured due to the extreme lateral loading applied to TL-6 barriers and the discontinuities associated with ends and expansion joints. Other methods may be needed to increase the capacity of concrete slabs at these discontinuous regions. Various options are available for anchoring and developing the vertical steel rebars within the concrete slab, which

provide tensile and moment capacity and shear transfer at the barrier's base. For now, it is suggested that the barrier's centerline be positioned within the ⅓-point and midpoint across the 12-ft wide concrete slab, or centered between 3 ft and 6 ft, respectively, using the larger lateral width on the traffic-side face of the barrier. For example, if the high-performance barrier is planned for roadside applications with the barrier centered at 3 ft from an exterior edge, the exposed slab width under the vehicle would be 9 ft less one-half of the barrier's width, or 8 ft - 1 in. For median applications,  the barrier's centerline would most often be placed near the centerline of the median slab.
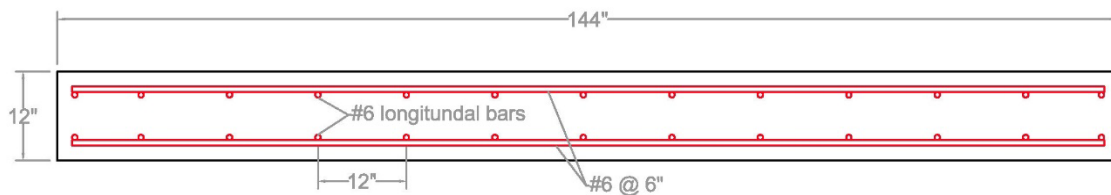


Figure 6.1 Interior Reinforced-Concrete Slab for TL-6 Roadside/Median Applications

For the grade beam option, a conservative design methodology that focused on torsional capacity was used. The design loads for the TL-6 barrier were multiplied by their application heights to obtain a design moment at the base of the barrier. This moment was taken as the design torsion load which the grade beam was configured to withstand. This methodology has been previously used to design grade beam foundations for TL-3 and TL-5 barrier systems [29-31], with only small changes made to the design procedure related to updated torsion capacity calculations found in *ACI 318* [32].

This conservative design methodology produced a reinforced-concrete grade beam foundation configuration for interior sections that measured 30-in. thick by 60-in. wide, as shown

in Figure 6.2. The interior section is reinforced with no. 6 transverse stirrups (i.e., closed loops)

spaced at 8 in. centers and 20 no. 6 longitudinal bars. For end sections adjacent to discontinuities,

the grade beam was increased in size to be 30-in. thick by 84-in. wide, as shown in Figure 6.3.

End section reinforcement consisted of no. 6 transverse stirrups (i.e., closed loop) at 6 in. centers

34 no. 6 longitudinal bars. Various options are available for anchoring and developing the

vertical steel rebars within the concrete grade beam, which provide tensile and moment capacity

and shear transfer at the barrier's base. For now, it is suggested that the barrier's centerline be

positioned approximately at the midpoint of the concrete grade beam in both roadside and

median applications.
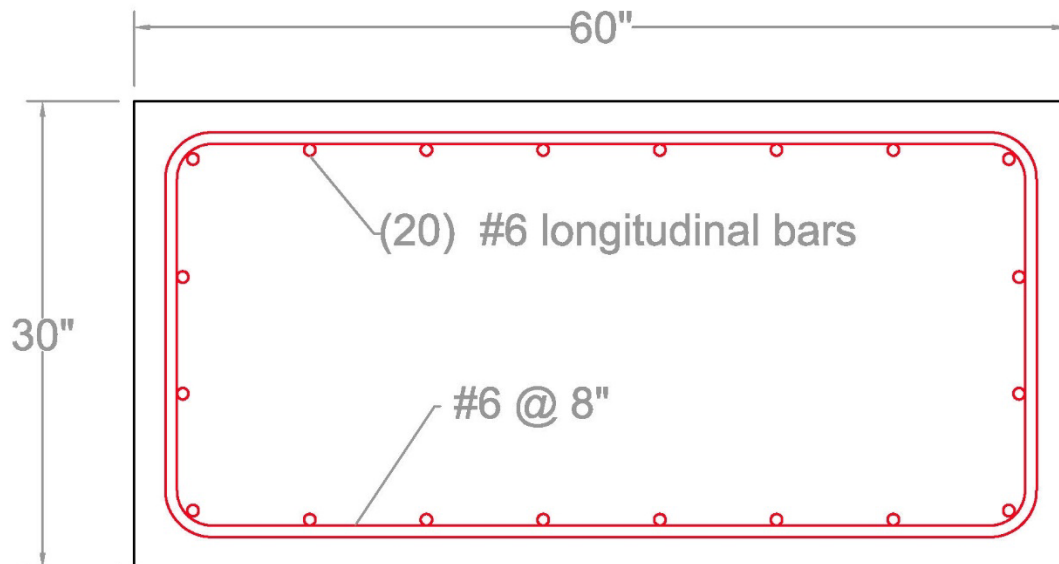


Figure 6.2 Interior Reinforced-Concrete Grade Beam for TL-6 Roadside/Median Applications
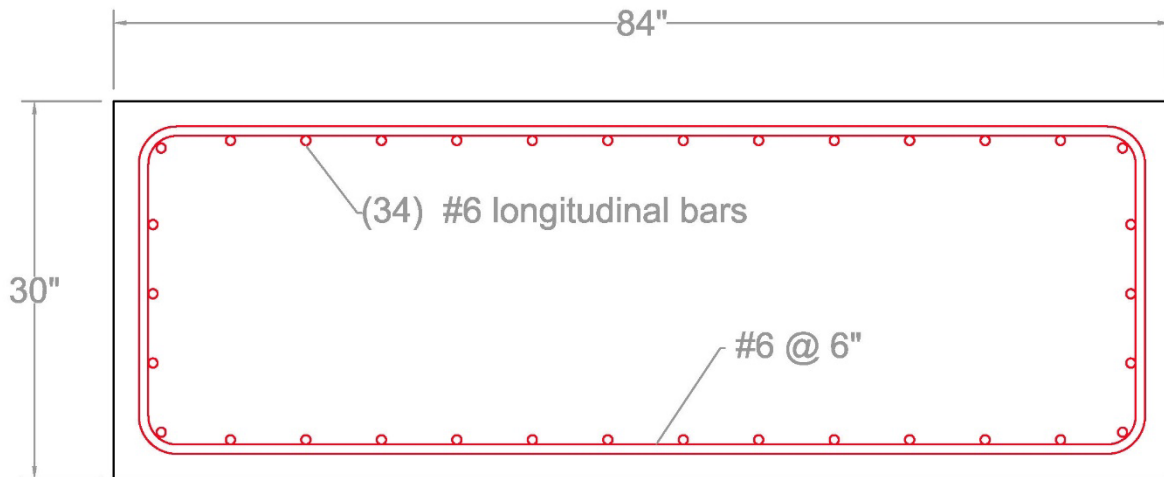
Figure 6.3 End Region Grade Beam for TL-6 Roadside/Median Applications

6.4 Bridge Railing Applications

As part of this design effort, the crash-tested, TL-6 barrier configuration was also adapted

for implementation as a bridge railing. The updated design methodology of NCHRP Report 1078

[33] was used to develop a bridge deck overhang configuration to support the barrier, and the

performance of the final configuration was estimated using static pushover simulations in LS-

DYNA. Designs were developed for both interior and end regions.

*6.4.1 Design Methodology*

In the design methodology presented in NCHRP Report 1078, the ultimate failure

mechanism in the barrier is characterized as a trapezoidal yield-line mechanism. The interior-

region mechanism is shown in Figure 6.4, and the corresponding equations for the critical length,

$L_c$, and redirective capacity, $R_w$, of the mechanism are shown in Equations 3 and 4, respectively.

In these equations, $L_t$ is the longitudinal length of load application (ft), $M_w$ is the vertical-axis

(wall) bending strength of the parapet (kip-ft), $M_{c,avg}$ and $M_{c,base}$ the average longitudinal-axis

(cantilever) bending strengths of the parapet over its height and at its base, respectively (kip-ft/ft), $H$ is the height of the barrier (ft), and $H_e$ is the load application height (ft).

$$L_c = L_t + \sqrt{8 \frac{M_w H}{M_{c,avg}}} \tag{3}$$

$$R_w = \frac{H}{H_e} \left( M_{c,base} \frac{L_t}{H} + M_{c,avg} \frac{L_c - L_t}{H} + M_w \frac{8}{L_c - L_t} \right) \tag{4}$$
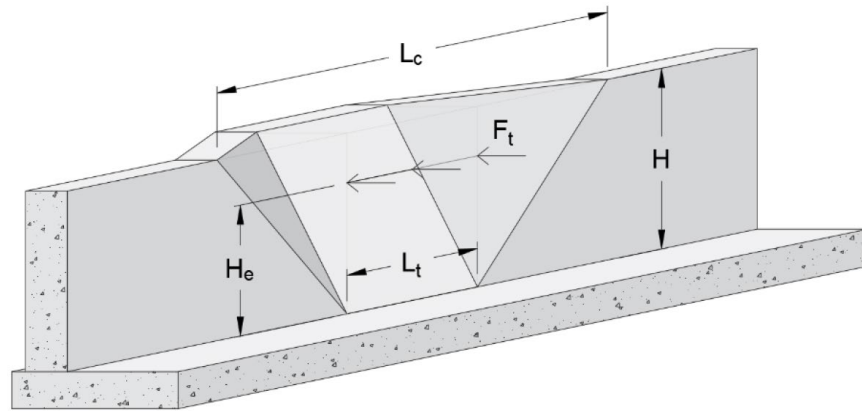


Figure 6.4 Parapet Yield-Line Mechanism (Interior Regions)

A barrier is typically considered to have adequate redirective capacity if the result of Equation 4, $R_w$, is greater than the lateral impact load, $F_t$. For this barrier, the assumed lateral impact load was a combination of a 200-kip load applied at the top of the barrier (62 in.) and a 100-kip load applied at the height of the rear axle (22 in.). The effective design load, then, was 300 kips applied at a weighted-average height of 48.7 in. For the median application, wherein it is assumed that the foundation has a greater bending capacity then the barrier at its base, the calculated redirective capacity of the barrier was 269 kips. Thus, when compared to the expected lateral load of 300 kips, the barrier was roughly 10% understrength, although this was deemed

acceptable due to expected inertial resistance and the conservative nature of the estimated demand.

For barriers with fixed bases, Equation 4 is an adequate predictor of static barrier capacity. However, a minor adjustment must be made in bridge railing applications, where the barrier is attached to a bridge deck overhang. If the transverse bending capacity of the bridge deck is less than that of the barrier at its base, then the full strength of the barrier cannot be developed along the horizontal yield-line. Therefore, in these cases, the bending strength along the horizontal yield-line must be taken as the bending strength of the bridge deck. The implications of this adjustment for the TL-6 bridge railing are discussed in the following section.

In order to design the bridge deck overhang, NCHRP Report 1078 was used. This resource includes a lateral-load-based method for estimating bridge deck overhang demands in which flexural demands are assumed to distribute according to the pattern shown in Figure 6.5. Flexural demands effectively distribute at a 45º angle with downward transmission through the parapet from the extents of the yield-line mechanism, then distribute at a 60º angle with inward transmission through the overhang. Using this effective distribution pattern, moment demands in the deck slab at Design Regions A-A, $M_{1A}$, and B-B, $M_{1B}$, are estimated using Equations 5 through 8. In these equations, $t_s$ is the deck thickness (ft), $L_{1A}$ is the effective distribution length at Design Region A-A (ft), $L_{1B}$ is the effective distribution length at Design Region B-B (ft), $X_{AB}$ is the distance between Design Regions A-A and B-B (ft), and $M_{sw,A}$ and $M_{sw,B}$ are dead-weight moments at Design Regions A-A and B-B (kip-ft/ft). The locations of Design Regions A-A and B-B are shown in Figure 6.6.
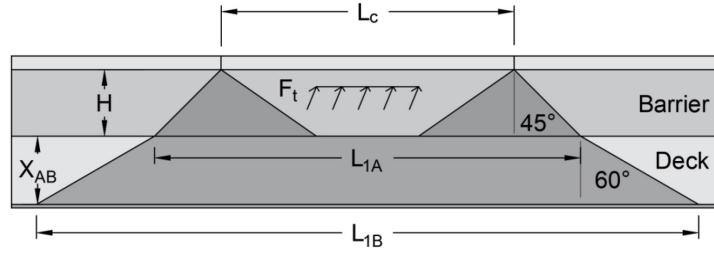
Figure 6.5 Distribution of Moment Demands through Barrier and Deck (Interior Regions)
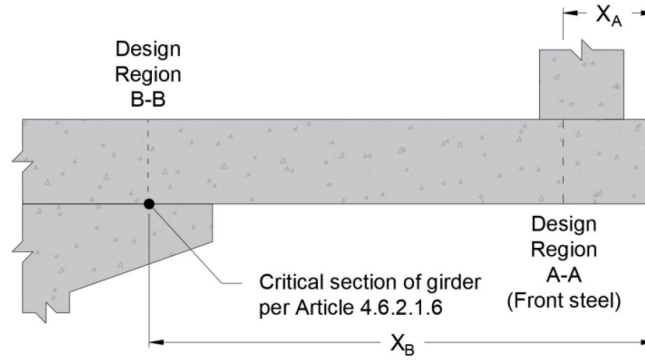


Figure 6.6 Location of Design Regions A-A and B-B in bridge deck overhang

$$L_{1A} = L_c + 2H \tag{5}$$

$$M_{1A} = \min \left\{ \begin{array}{c} M_{c,base} \\ \dfrac{F_t(H_e + 0.5t_s)}{L_{1A}} \end{array} \right\} + M_{sw,A} \tag{6}$$

$$L_{1B} = L_{1A} + 2X_{AB} \tan 60° \tag{7}$$

$$M_{1B} = \dfrac{F_t(H_e + 0.5t_s)}{L_{1B}} + M_{sw,B} \tag{8}$$

For impacts at end regions, where both the barrier and bridge deck terminate, a different

yield-line mechanism is used. This mechanism is shown in Figure 6.7, and the corresponding

critical length and static capacity are calculated via Equations 9 and 10. For the TL-6 barrier on a

rigid base, the estimated static capacity was 312 kips.

$$L_c = \frac{1}{8M_{c,avg}}\left(5M_{c,avg}L_t + \sqrt{M_{c,avg}\left(M_{c,avg}L_t^2 + 4M_{c,base}L_t^2 + 128M_wH\right)}\right) \qquad 9)$$

$$R_w = \frac{H}{H_e}\left(3 + \frac{L_c - L_t}{L_c - 0.5L_t}\right)^{-1}\left(\frac{8M_w}{L_c - 0.5L_t} + \frac{4M_{c,avg}(L_c - 0.5L_t)}{H} + \frac{2M_{c,base}L_t}{H}\right) \qquad (10)$$
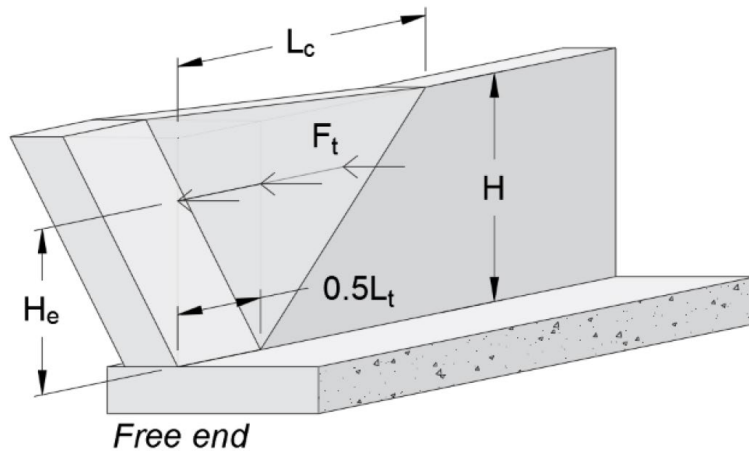


Figure 6.7 Parapet Yield-Line Mechanism (End Regions)

To estimate bridge deck flexural demands at end regions, a pattern which is similar to

that used for interior regions is used. However, at end regions, load distribution is restricted to

one direction. Bridge deck flexural demands at the end region were estimated using the pattern

shown in Figure 6.8 and Equations 11 through 13.
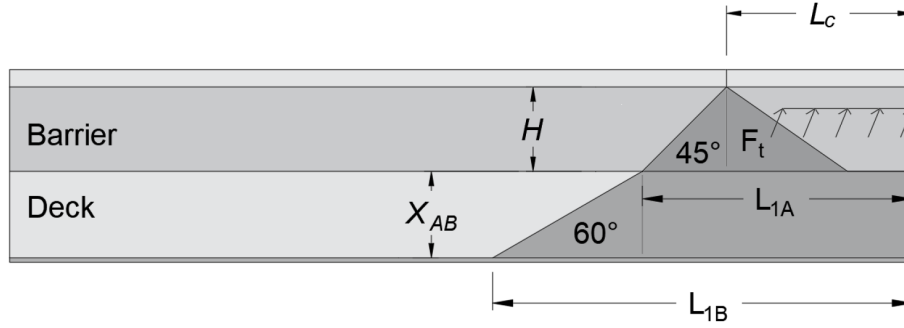
Figure 6.8 Distribution of Moment Demands through Barrier and Deck (End Regions)

$$L_{1A} = L_c + H \tag{11}$$

$$M_{1A} = \min \left\{ \begin{array}{c} M_{c,base} \\ \dfrac{F_t(H_e + 0.5t_s)}{L_{1A}} \end{array} \right\} + M_{sw,A} \tag{12}$$

$$L_{1B} = L_{1A} + X_{AB} \tan 60^o \tag{13}$$

$$M_{1B} = \frac{F_t(H_e + 0.5t_s)}{L_{1B}} + M_{sw,B} \tag{14}$$

For both interior and end regions, tensile demands in the bridge deck do not distribute effectively. These demands, which are exerted on the bridge deck as shears at the base of the railing, remain concentrated below the load application region. Thus, for all regions, the tensile demand in the deck, $N$, is calculated via Equation 15 (kips/ft). The effect of lateral deck tension was considered as a penalty on the available area of transverse steel when calculating the bending capacity of the bridge deck.

$$N = \frac{F_t}{L_t} \tag{15}$$

It should be noted that NCHRP Report 1078 includes a bridge deck shear capacity evaluation below the railing. As this evaluation is system-specific, it is discussed in the following section.

*6.4.2 Recommended Bridge Deck Overhang Design Configurations*

The recommended configuration for implementation of the TL-6 barrier in bridge railing applications, which was developed using the NCHRP Report 1078 methodology, is shown in Figure 6.9 for interior and end regions. The critical length of the end-region yield-line mechanism in the barrier was roughly 13 ft, and it was assumed that flexural demands distribute at 45° with downward transmission through the barrier. Thus, the effective length of bridge deck participating in end-region behavior was roughly 18 ft. For this system, an "end region" can therefore be conservatively considered to be any region located within 20 ft of an expansion joint or free end of the barrier and bridge deck.

$f'_c$ = 5 ksi
$f_y$ = 60 ksi

*Interior Regions*
*(More than 20 ft from free end)*

*End Regions*
*(Within 20 ft of free end)*
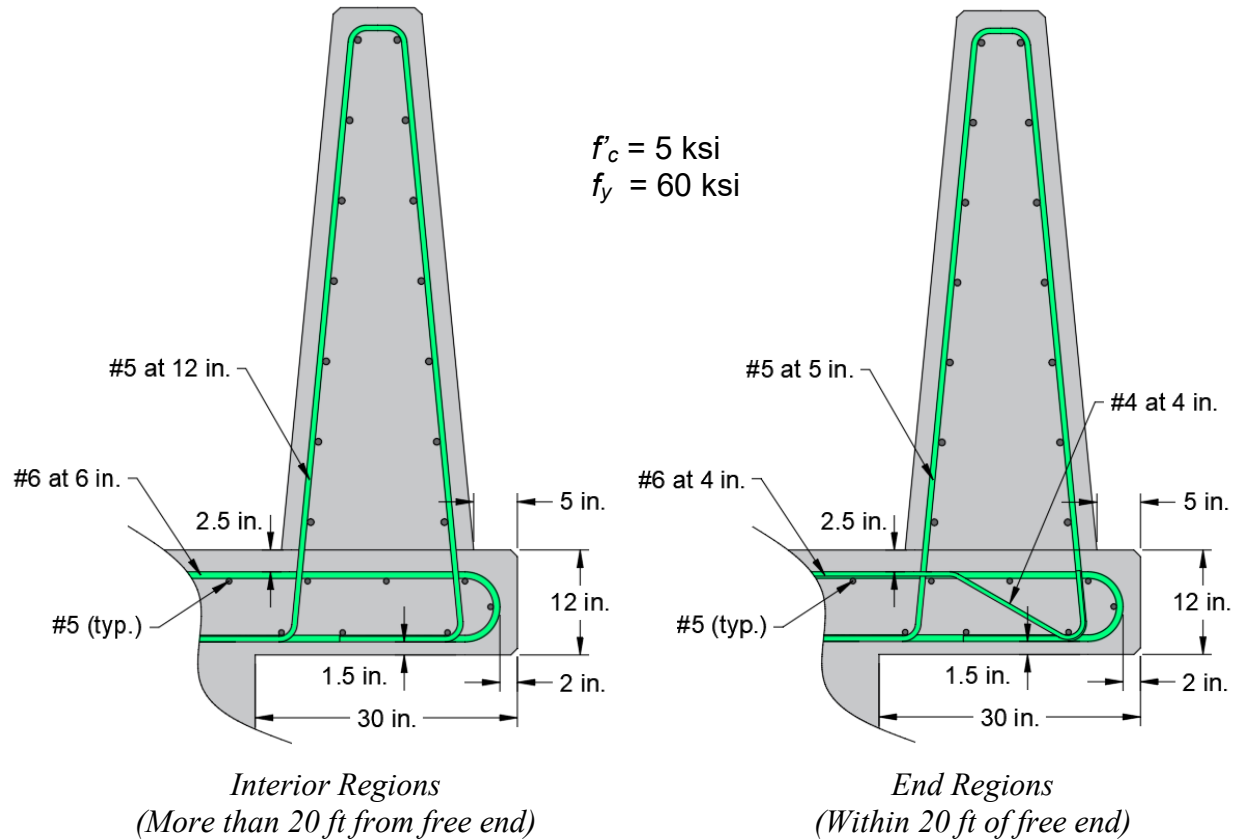
Figure 6.9 Recommended TL-6 Parapet Railing and Bridge Deck Configuration

Slab thickness and transverse reinforcement are the primary design parameters affecting bridge deck performance during railing impacts. However, prior to designing the slab for strength, basic design choices reflecting best practices were established. First, hooked transverse slab bars were specified. Hooking transverse bars results in improved transverse bar development, provides concrete confinement under the barrier, and may encourage a strut-and-tie mechanism for load transfer through the slab joint. Additionally, a substantial top cover (2.5 in.) was specified for durability, particularly for protection against de-icing agents and vehicle wear. Lastly, a 5-in. edge distance was specified to ensure that the concentrated compressive demand exerted by the barrier was located over the straight portion of the transverse deck bars.

Barrier compressive regions which are centered over the hooked portion of the bars or over unreinforced concrete may result in field cover spalling.

Many of the baseline design preferences described above were intended to reduce the likelihood of the bridge deck experiencing cover spalling, diagonal tension failure, and delamination. These common damage mechanisms have been observed in several physical tests of bridge decks supporting concrete parapet railings, including an end-region impact test performed under NCHRP Project 12-119, which is shown in Figure 6.10.



Figure 6.10 Damage in bridge deck supporting concrete parapet railing

For both the interior and end regions, a slab thickness of 12 in. was specified. This thickness is within the typical range for most state departments of transportation and is sufficiently thick for embedment of the vertical barrier bars. For additional anchoring, vertical barrier bars were hooked around longitudinal slab steel. Pull-out testing performed by the Florida

August 7, 2024

MwRSF Report No. **Error! Reference source not found.**

DOT has suggested that bars which hook around perpendicular reinforcement can be developed over distances which are significantly less than their code development length [34].

For interior regions, the barrier's cantilever bending strength at its base is 33 kip-ft/ft, and the concentrated downward force acting on the bridge deck is 37 kips/ft. The estimated flexural demand acting on the bridge deck based on the lateral impact load is 34 kip-ft/ft. As this value is greater than the cantilever bending capacity of the barrier, the strength of the barrier is taken as the effective bridge deck flexural demand. The design tension demand on the slab is 30 kips/ft.

Local, diagonal tension damage under the railing is not expected for interior regions. The downward compressive force acting at the back of the railing at its ultimate strength is 37 kips/ft. While the basic shear capacity of the slab is only 20 kips/ft, the use of hooked transverse bars and 5-in. edge distance is expected to encourage load transfer through the joint via a strut-and-tie mechanism, rather than through direct shear. The strut-and-tie capacity of the bridge deck calculated using the recommendations of NCHRP Report 1078 is greater than the demand of 37 kips/ft.

An acceptable bridge deck capacity was achieved for interior regions using #6 bars spaced at 6 in., which results in a transverse pure bending strength of 39 kip-ft/ft. When accounting for design tension demand of 30 kips/ft, the transverse bending strength of the slab is reduced to 29 kip-ft/ft. Thus, the final bridge deck configuration is roughly 12% understrength according to NCHRP Report 1078 procedures. Limited deck damage may occur, but the barrier-deck system is expected to be sufficiently robust, that its capability to contain and redirect the tractor-tank trailer will not be compromised. Reducing the transverse bar spacing was not desired, as using a 6-in. spacing allows for every other transverse bar to be tied directly to vertical barrier steel. It should be noted that, as the deck slab has a lower flexural strength than the barrier at its base, the yield-line capacity of the barrier required slight adjustment. When

limiting the strength of the horizontal yield-line mechanism to the deck bending strength of 29 kip-ft/ft, the estimated barrier capacity was reduced from 269 kips to 262 kips.

For end regions, the barrier's cantilever bending strength at its base is 73 kip-ft/ft, and the concentrated downward force acting on the bridge deck is 68 kips/ft. The estimated flexural demand acting on the bridge deck based on the lateral impact load is 75 kip-ft/ft. As was true for the interior region, this value is greater than the cantilever bending capacity of the barrier. Thus, the flexural demand in the deck is taken as the bending strength of the barrier, as that is the maximum moment which can be transferred to the slab. The design tension demand on the slab is 30 kips/ft, which is unchanged from the interior region.

Due to the extreme compressive load exerted at the back face of the barrier of 68 kips/ft, the bridge deck is likely to develop diagonal tension damage below the railing if the barrier is loaded to its limit. Thus, diagonal steel consisting of #4 bars spaced at 4 in. was specified to provide resistance against shear damage and/or compression strut splitting in the region below the barrier. Physical testing has not confirmed whether these bars could be developed for effective resistance against local failure in this region.

Given the magnitude of the barrier's bending capacity at end regions, there is no reasonable transverse steel configuration which meets the requirements of NCHRP Report 1078 for structural adequacy. The flexural demand at the base of the barrier in end regions is 73 kip-ft/ft. Using #6 bars spaced at 4 in. results in a slab pure bending capacity of 72 kip-ft/ft. However, after accounting for lateral deck tension and expected concrete damage below the rail, the estimated bending strength of the slab is 51 kip-ft/ft. Thus, at end regions, the configuration shown is roughly 30% understrength according to NCHRP Report 1078 procedures. Despite this understrength, this design is still presented as an acceptable configuration due to additional sources of capacity not included in the analysis procedure, such as inertia, strain hardening, and

material strain rate effects. Further, it is anticipated that damage to the system would result in a distribution of impact loads to adjacent, undamaged regions, rather than a sudden and catastrophic failure of the parapet.

Additional measures, although atypical for roadside hardware, could be taken to reduce the likelihood of bridge deck damage and improve the performance of the system at both interior and end regions. Most notably, transverse reinforcement in the bridge deck could be specified as Gr. 80, rather than Gr. 60. Recent internal reviews and correspondence have suggested that the cost difference between Gr. 80 and Gr. 60 reinforcing steel is minor. Secondly, a greater concrete compressive strength could be specified. Results shown herein correspond to 5-ksi concrete; specifying 6- or 7-ksi concrete would significantly reduce the risk of local concrete damage below the railing, improving the overall performance of the system in the event of a design impact.

*6.4.3 Bridge Railing Simulation Results*

Static pushover simulations of recommended railing and deck configurations were executed in LS-DYNA to estimate their performance. For conservatism and consistency with design assumptions, models used 5-ksi concrete and 60-ksi elastic-perfectly plastic reinforcing steel. Load was applied as a prescribed displacement of 4 in. over a duration of 1 sec, a length of 10 ft, and a height of 48.7 in. Material rate effects were disabled, and the rate of displacement was sufficiently slow as to mitigate inertial effects. A basic model summary is shown in Figure 6.11.

100-ft span

*Load application*
4 in. over 1 sec
$L_t$ = 10 ft
$H_e$ = 48.7 in.

Free interface
(separate pours)

*Materials*
$f'_c$ = 5 ksi
$f_y$ = 60 ksi

Fixed boundary
condition along
slab interior
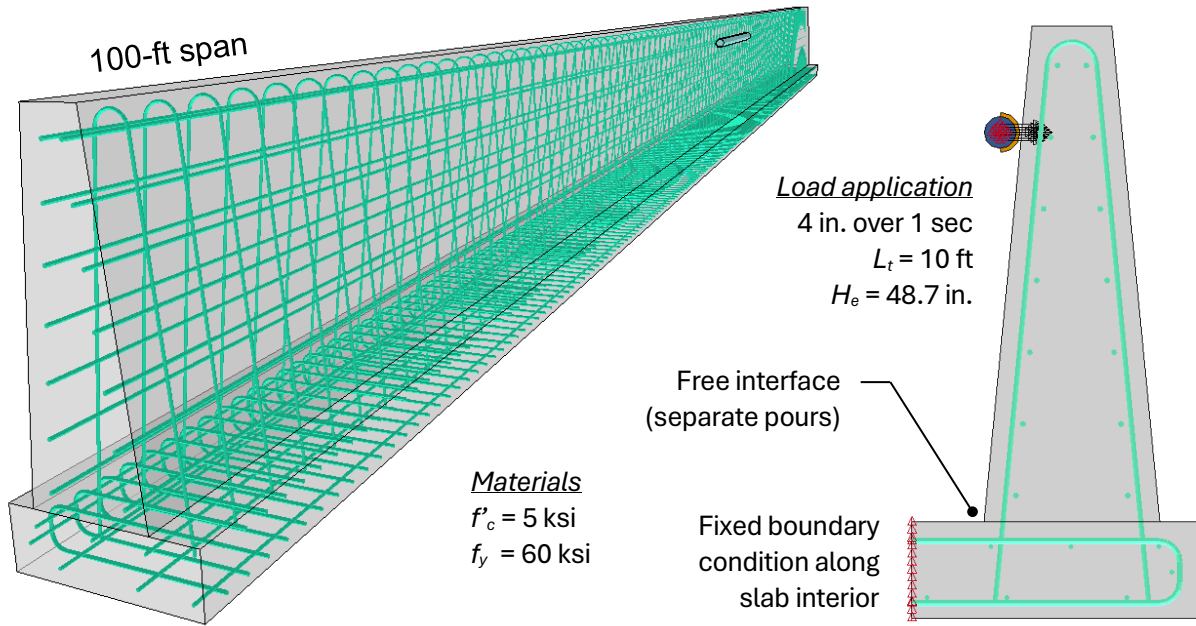
Figure 6.11 LS-DYNA Model Description

Results from the interior and end-region pushover simulations, including force-deflection response and concrete damage at the peak load, are shown in Figure 6.12 and Figure 6.13, respectively. As shown, the NCHRP Report 1078 methodology was a reasonable predictor of bridge railing and deck behavior. Peak static loads exerted by the railing for interior and end-region loading were 264 kips and 267 kips, respectively. Deck damage was more significant in the end-region loading simulation due to the increased magnitude of the concentrated compressive force at the back face of the barrier. In both cases, modeling results suggested that the TL-6 barrier would perform adequately in bridge railing applications using the recommended bridge deck configurations. However, significant bridge deck damage may occur for design impacts at end regions. Thus, applying special treatments to end regions of the slab, such as propping or selective thickening, should be considered if deck damage is impermissible.
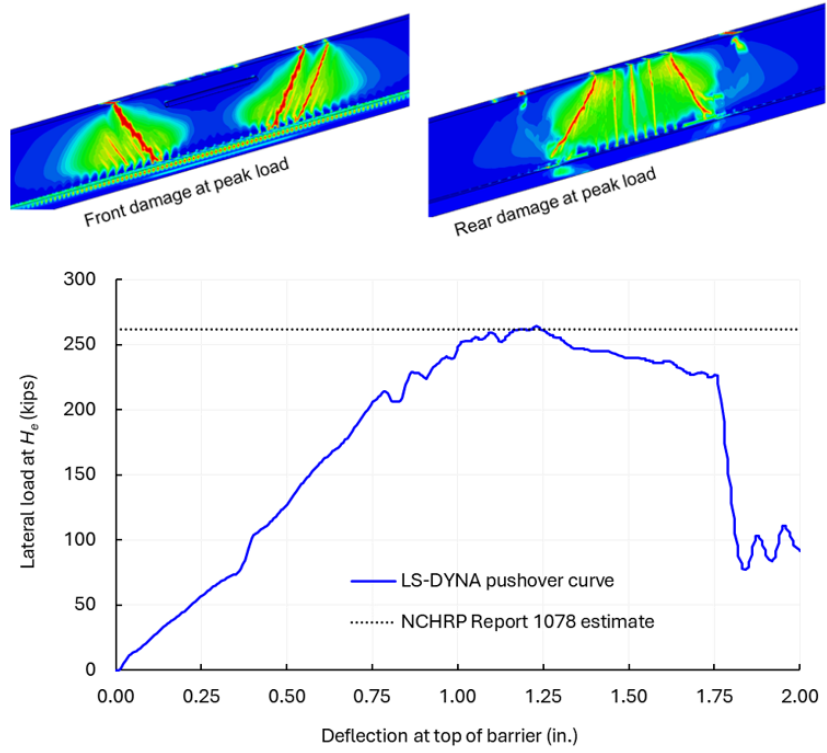
Figure 6.12 Interior-Region Static Pushover Simulation Results
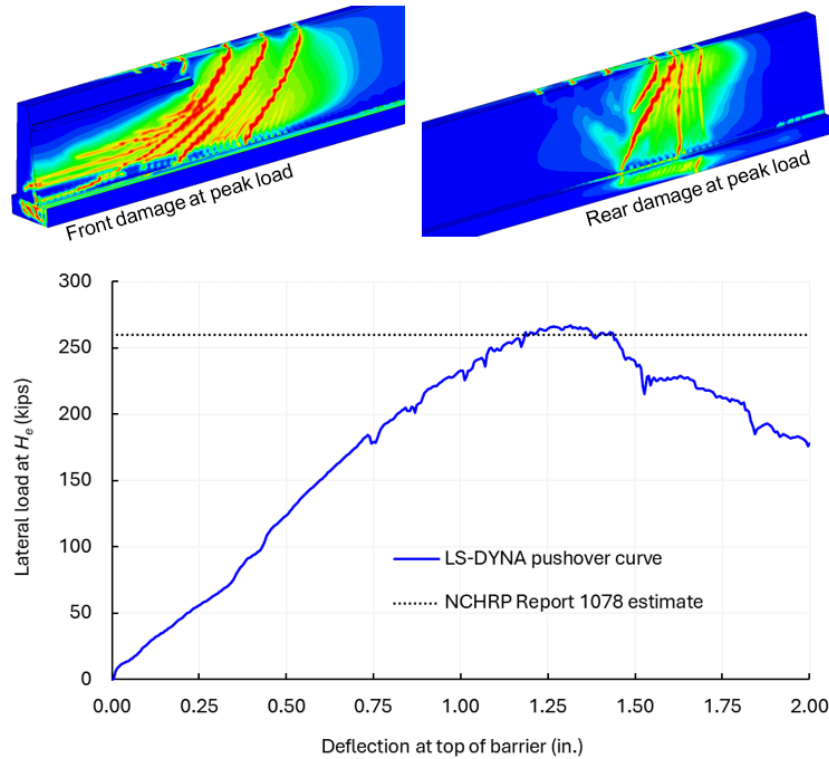
Figure 6.13 End-Region Static Pushover Simulation Results

## 6.5 Example Height Transition Details for Concrete End Sections

For the implementation of the high-performance, 62-in. tall, reinforced-concrete, single-slope barrier system, it will be necessary to eventually install end sections. These end sections will allow for the top barrier height to be gradually transitioned from 62 in. to a common buttress height of 32 in. Typically, end sections are either shielded with crashworthy impact attenuators (i.e., crash cushions) or protected through the attachment of a crashworthy, thrie-beam approach guardrail transition, which often connects corrugated, W-beam guardrail systems to concrete end sections or buttresses. MASH TL-3 crash cushions and approach guardrail transitions are readily available for use in shielding blunt-end concrete barrier sections, resulting from terminations of bridge railings as well as roadside and median barriers. To assist with the implementation of the TL-6 barrier system, conceptual barrier height transitions have been provided for use at these end

regions. However, steel reinforcement details have been omitted to allow for end users to create their own geometries and structural details.

Two examples have been provided to transition the 62-in. tall, single-slope concrete barrier system to a 32-in. tall, concrete end section (i.e., standardized buttress) – one detail for roadside applications and one detail for median applications, which are shown in Figure 6.14 and Figure 6.15, respectively. Note that the standardized buttress segment was previously developed, crash tested, and evaluated for use with a MASH TL-3 thrie-beam approach guardrail transition system [35].
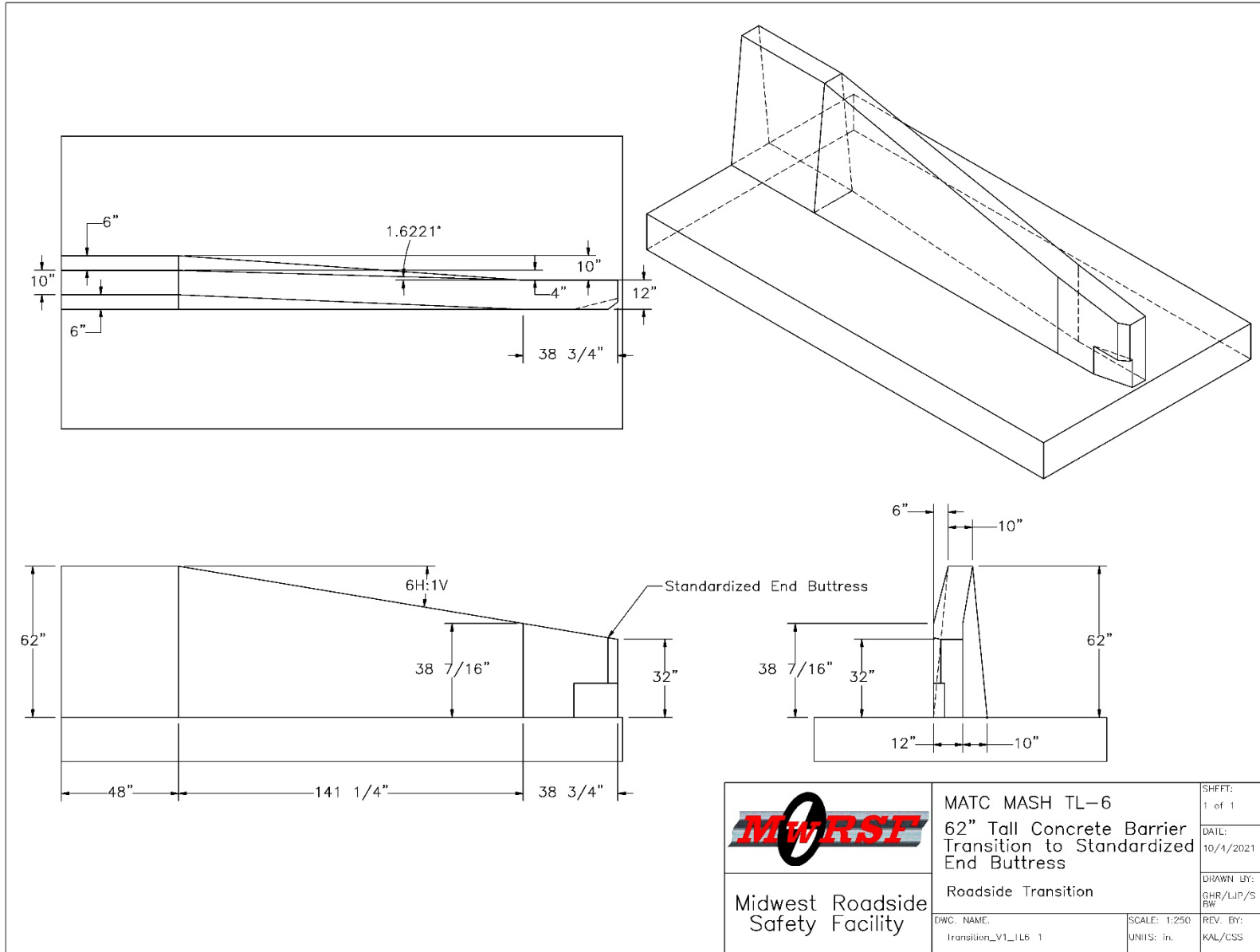
Figure 6.14 Example Barrier Height Transition - Roadside Applications
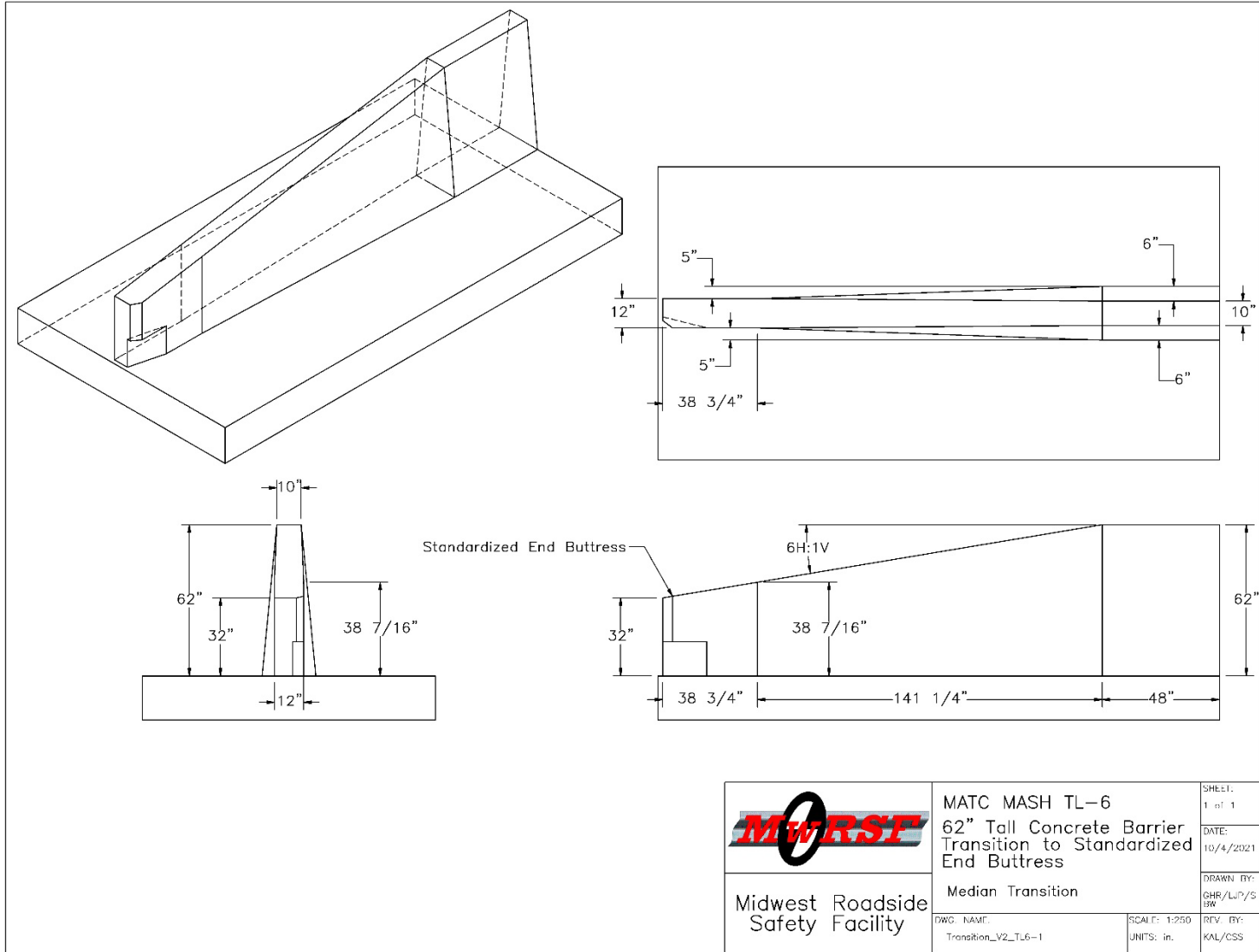
Figure 6.15 Example Barrier Height Transition - Median Applications

References

1.  Ross, H.E., Sicking, D.L., Zimmer, R.A., and Michie, J.D., *Recommended Procedures for the Safety Performance Evaluation of Highway Features*, National Cooperative Highway Research Program (NCHRP) Report 350, Transportation Research Board, Washington, D.C., 1993.

2.  *Manual for Assessing Safety Hardware (MASH)*, First Edition, American Association of State Highway and Transportation Officials (AASHTO), Washington, D.C., 2009.

3.  *Manual for Assessing Safety Hardware (MASH), Second Edition*, American Association of State Highway and Transportation Officials (AASHTO), Washington, D.C., 2016.

4.  Hirsch, T.J., and W.L. Fairbanks. *Bridge Rail to Restrain and Redirect 80,000-lb Tank Trucks*, Report FHWA/TX-84/911-1F, Texas Transportation Institute, College Station, Texas, January 1984.

5.  Dong, C., Q. Dong. B. Huang, W. Hu, and S.S. Nambisan, Estimating Factors Contributing to Frequency and Severity of Large Truck-Involved Crashes, *Journal of Transportation Engineering, Part A: Systems*, American Society of Civil Engineers, 143(8), DOI: 10.1061/JTEPBS.0000060, 2017.

6.  Shen, X., Y. Yan, X. Li, C. Xie, and L. Wang, Analysis of Tank Truck Accidents Involved in Road Hazardous Materials Transportation in China, *Journal of Traffic Injury Prevention*, 15(7): 762-768, DOI: https://doi.org/10.1080/15389588.2013.871711, 2014.

7.  McKnight, A.J. and G.T. Bahouth, Analysis of Large Truck Rollover Crashes, *Journal of Traffic Injury Prevention*, 10(5), 421-426, DOI: 10.1080/15389580903135291, 2009.

8.  Iranitalab, A., A. Khattak, and G. Bahouth, Statistical Modeling of Cargo Tank Truck Crashes: Rollover and Release of Hazardous Materials, *Journal of Safety Research*, National Safety Council and Elsevier, 74: 71-29, DOI: https://doi.org/10.1016/j.jsr.2020.04.010, 2020.

9.  Lyu, S., S. Zhang, S. Huang, S. Peng, and J. Li, Investigating and Modeling of the LPG Tank Truck Accident in Wenling, China, *Process Safety and Environmental Protection*, 157: 493-508, https://doi.org/10.1016/j.psep.2021.10.022, 2022

10. *Highway Accident Report - Transport Company of Texas, Tractor-semitrailer (Tank) Collision with Bridge Column and Sudden Dispersal of Anhydrous Ammonia Cargo, I-610 at Southwest Freeway*, Report Number: NTSB-HAR-77-1, National Transportation Safety Board, Washington, D.C., April 14, 1977.

11. *Highway Accident Brief*, Accident Number: HWY-04-MH-012, National Transportation Safety Board, Washington, D.C.

12.   *Rollover of a Truck-Tractor and Cargo Tank Semitrailer Carrying Liquefied Petroleum Gas and Subsequent Fire*, Accident Report Number: NTSB/HAR-11/01 PB2011-916201, National Transportation Safety Board, Washington, D.C.

13.   CBS News Los Angeles, *Tanker Truck Crash Spills 9,000 Gallons Of Fuel In Banning, All Lanes Of Interstate 10 Shut Down For Hours*, August 31, 2021, https://www.cbsnews.com/losangeles/news/tanker-truck-crash-spills-9000-gallons-fuel-banning-all-lanes-interstate-10-shut-down-hours/.

14.   Whitfield D.L., Schmidt J.D., Faller R. K., and Steelman J. S., *Investigation and Development of a Test Level 6 Barrier - Phase I*, Report No. TRP-03-404-18, MwRSF, University of Nebraska-Lincoln, Lincoln, Nebraska, October 2018.

15.   Whitfield, D.L., *Investigation of a Tractor-Tank Trailer Roadside Containment Barrier*, Master's Thesis, University of Nebraska-Lincoln, Lincoln, Nebraska, November 2018.

16.   Rasmussen J.D., Stolle C.S., R.K. Faller, J.S. Steelman, E. Vasquez, and S.H., Yoo., *Investigation and Development of a Test Level 6 Barrier - Phase II*, Report No. TRP-03-430-20, MwRSF, University of Nebraska-Lincoln, Lincoln, Nebraska, January 2020.

17.   Rasmussen J.D., C.S. Stolle, R.K. Faller, J.S. Steelman, and E. Vasquez, *Investigation and Development of a Test Level 6 Barrier - Phase III*, Report No. TRP-03-457-21, MwRSF, University of Nebraska-Lincoln, Lincoln, Nebraska, October 2021.

18.   Vasquez, E,. *Fluid Modeling and Analysis for a MASH TL-6 Vehicle Model*, Master's Thesis, Mechanical Engineering, University of Nebraska-Lincoln, December 2020.

19.   Mak K.K, Beason W.L., Hirsch T.J., and Campise W.L, *Oblique Angle Crash Test of Loaded Heavy Trucks into an Instrumented Wall*, Report No. DOT HS 807 256, Texas Transportation Institute, Texas A&M University, 1988.

20.   C.S. Stolle, Faller, R.K., Vasquez, E., Bielenberg, R.W., Fang, C., Rosenbaugh, S.K., Loken, A.E., Revell, J.R., Steelman, J., and Habib, Z., *MASH TL-6 Evaluation of a 62-In. Tall, Single-Slope, Concrete Median Barrier - Phase IV*, Report No. TRP-03-463-23, MwRSF, University of Nebraska-Lincoln, Lincoln, Nebraska, July 25, 2023.

21.   Rosenbaugh, S.K., D.L. Sicking, and R.K. Faller, *Development of a TL-5 Vertical Faced Concrete Median Barrier Incorporating Head Ejection Criteria*, Report No. TRP-03-194-07, Midwest Roadside Safety Facility, University of Nebraska-Lincoln, Lincoln, Nebraska, December 2007.

22.   Mak, K.K. and D.L. Sicking, *Rollover Caused by Concrete Safety Shaped Barrier*, Transportation Research Record No. 1258, Transportation Research Board, National Research Council, Washington, D.C., 1990.

23.   Albuquerque, F.D.B and D.L. Sicking, *Evaluation of the In-Service Safety Performance of Safety-Shape and Vertical Concrete Barriers*, Report No. TRP-03-259-11, MwRSF, University of Nebraska-Lincoln, Lincoln, Nebraska, December 2011.

24. AASHTO, *AASHTO LRFD Bridge Design Specifications*, 9th Edition, Washington, D.C., 2020.

25. Jeon, S., M. Choi, and Y. Kim, *Ultimate Strength of Concrete Barrier by the Yield Line Theory*, International Journal of Concrete Structures and Materials, Vol. 2, June 2008.

26. Bielenberg, R.W., Dowler, N.T., Faller, R.K., and Urbank, E.L., *Crash Testing and Evaluation of the HDOT 42-in. Tall, Aesthetic Concrete Bridge Rail: MASH Test Designation Nos. 3-10 and 3-11*, Report No. TRP-03-424-20, MwRSF, University of Nebraska-Lincoln, Lincoln, Nebraska, January 9, 2020.

27. Moran, S.M., Bligh, R.P., Menges, W.L., Schroeder, W., and Kuhn, D., *MASH Test 4-12 of Shallow Anchorage Single Slope Traffic Rail (STTR)*, Test Report No. 0-6968-R10, Texas A&M Transportation Institute, Texas A&M University, College Station, Texas, December 2020.

28. Sheikh, N.M., Kovar, J.C., Cakalli, S., Menges, W.L., Schroeder, G.E., and Kuhn, D.L., *Analysis of 54-In. Tall Single-Slope Concrete Barrier on a Structurally Independent Foundation*, Test Report No. 0-6948-R1, Texas A&M Transportation Institute, Texas A&M University, College Station, Texas, September 2019.

29. Rosenbaugh, S.K., Faller, R.K., Hascall, J.A., Allison, E.A., Bielenberg, R.W., Rohde, J.R., Polivka, K.A., Sicking, D.L., and Reid, J.D., *Development of a Stand Alone Concrete Bridge Pier Protection System*, Report No. TRP-03-190-08, MwRSF, University of Nebraska-Lincoln, Lincoln, Nebraska, April 18, 2008.

30. Rosenbaugh, S.K., Sicking, D.L., and Faller, R.K., *Development of a TL-5 Vertical Faced Concrete Median Barrier Incorporating Head Ejection Criteria*, Report No. TRP-03-194-07, MwRSF, University of Nebraska-Lincoln, Lincoln, Nebraska, December 10, 2007.

31. Rosenbaugh, S.K., Schmidt, J.D., Regier, E.M., and Faller, R.K., *Development of the Manitoba Constrained-Width, Tall Wall Barrier*, Report No. TRP-03-356-16, MwRSF, University of Nebraska-Lincoln, Lincoln, Nebraska, September 26, 2016.

32. ACI Committee 318, *Building Code Requirements for Structural Concrete (ACI 318-19)*, American Concrete Institute, Farmington Hills, Michigan, 2019.

33. National Academies of Sciences, Engineering, and Medicine, *MASH Railing Load Requirements for Bridge Deck Overhang*. NCHRP Report No. 1078, Washington, D.C., The National Academies Press, https://doi.org/10.17226/27422, 2023.

34. Ansley, M., *Pull-out Test on Barrier Reinforcing*, Technical Memorandum, Florida Department of Transportation, March 2002.

35. Rosenbaugh, S.K., Faller, R.K., Asselin, N., and Hartwell, J., *Development of a Standardized Buttress for Approach Guardrail Transitions*, Report No. TRP-03-369-20, MwRSF, University of Nebraska-Lincoln, Lincoln, Nebraska, November 10, 2020.